Relaxation and frequency shifts induced by quasiparticles in superconducting qubits

G. Catelani, R. J. Schoelkopf, M. H. Devoret, and L. I. Glazman
Departments of Physics and Applied Physics, Yale University, New Haven, CT 06520, USA
(Dated: June 7, 2011)

As low-loss non-linear elements, Josephson junctions are the building blocks of superconducting qubits. The interaction of the qubit degree of freedom with the quasiparticles tunneling through the junction represent an intrinsic relaxation mechanism. We develop a general theory for the qubit decay rate induced by quasiparticles, and we study its dependence on the magnetic flux used to tune the qubit properties in devices such as the phase and flux qubits, the split transmon, and the fluxonium. Our estimates for the decay rate apply to both thermal equilibrium and non-equilibrium quasiparticles. We propose measuring the rate in a split transmon to obtain information on the possible non-equilibrium quasiparticle distribution. We also derive expressions for the shift in qubit frequency in the presence of quasiparticles.

PACS numbers: 74.50.+r, 85.25.Cp

I. INTRODUCTION

The operability of a quantum device as a qubit requires long coherence times in comparison to the gate operation time.[1] Over the years, longer coherence times in superconducting qubits have been achieved by designing new systems in which the decoupling of the quantum oscillations of the order parameter from other low-energy degrees of freedom is enhanced. For example, in a transmon qubit[2] the sensitivity to background charge noise is suppressed relative to that of a Cooper pair box. Irrespective of the particular design, in any superconducting device the qubit degree of freedom can exchange energy with quasiparticles. This intrinsic relaxation mechanism is suppressed in thermal equilibrium at temperatures much lower than the critical temperature, due to the exponential depletion of the quasiparticle population. However, both in superconducting qubits[3] and resonators[4] nonequilibrium quasiparticles have been observed which can lead to relaxation even at low temperatures. In this paper we study the quasiparticle relaxation mechanism in qubits based on Josephson junctions, both for equilibrium and nonequilibrium quasiparticles.

Quasiparticle relaxation in a Cooper pair box was considered in Ref. 5. In this system the charging energy is large compared to the Josephson energy and quasiparticle poisoning[6,7] is the elementary process of relaxation: a quasiparticle entering the Cooper pair box changes the parity (even or odd) of the state, bringing the qubit out of the computational space consisting of two charge states of the same parity. More recently the theory of Ref. 5 was extended to estimate the effect of quasiparticles in a transmon.[2] In this case the dominant energy scale is the Josephson energy, so that quantum fluctuations of the phase are relatively small, while the uncertainty of charge in the qubit states is significant. As mentioned above, the advantage of the transmon is its low sensitivity to charge noise. The possible role of nonequilibrium quasiparticles in superconducting qubits was investigated in Ref. 3. While the properties of many superconducting qubits – the phase and flux qubits,[8] the split transmon, and the newly developed fluxonium[9] – can be tuned by an external magnetic flux, the effect of the latter on the quasiparticle relaxation rate has not been previously analyzed. Elucidating the role of flux is the main goal of this work. In particular, we show that studying the flux dependence of the relaxation rate can provide information on the presence of nonequilibrium quasiparticles.

The paper is organized as follows: in the next section we present results for the admittance of a Josephson junction and the general approach to calculate the decay rate and energy level shifts due to quasiparticles in a qubit with a single Josephson junction. In Sec. III we consider a weakly anharmonic qubit, such as phase qubit or transmon, and relate its decay rate, quality factor, and frequency shift to the admittance of the junction. The cases of a Cooper pair box (large charging energy) and of a flux qubit with large Josephson energy are examined in Sec. IV. Some of the results presented in Secs. II-IV have been reported previously[10] in a brief format. In Sec. V we describe the generalization to multi-junction systems and study, as concrete examples, the two-junction split transmon and the many-junction fluxonium. We summarize the present work in Sec. VI. Throughout the paper, we use units $\hbar = k_B = 1$ (except otherwise noted).

II. GENERAL THEORY FOR A SINGLE-JUNCTION QUBIT

We consider a Josephson junction closed by an inductive loop, see Fig.1. The low-energy effective Hamiltonian of the system can be separated into three parts

$$\hat{H} = \hat{H}_\varphi + \hat{H}_{\rm qp} + \hat{H}_T\,. \tag{1}$$

The first term determines the dynamics of the phase degree of freedom in the absence of quasiparticles

$$\hat{H}_\varphi = 4E_C\left(\hat{N}-n_g\right)^2 - E_J\cos\hat{\varphi} + \frac{1}{2}E_L(\hat{\varphi}-2\pi\Phi_e/\Phi_0)^2\,, \tag{2}$$

where $\hat{N} = -id/d\varphi$ is the number operator of Cooper pairs passed across the junction, n_g is the dimensionless gate voltage, Φ_e is the external flux threading the loop, $\Phi_0 = h/2e$ is the flux quantum, and the parameters characterizing the qubit are the charging energy E_C, the Josephson energy E_J, and the inductive energy E_L.

The second term in Eq. (1) is the sum of the BCS Hamiltonians for quasiparticles in the leads

$$\hat{H}_{\rm qp} = \sum_{j=L,R} \hat{H}^j_{\rm qp}\,, \quad \hat{H}^j_{\rm qp} = \sum_{n,\sigma} \epsilon^j_n \hat{\alpha}^{j\dagger}_{n\sigma}\hat{\alpha}^j_{n\sigma}, \qquad (3)$$

where $\hat{\alpha}^j_{n\sigma}(\hat{\alpha}^{j\dagger}_{n\sigma})$ are quasiparticle annihilation (creation) operators and $\sigma =\uparrow,\downarrow$ accounts for spin. The quasiparticle energies are $\epsilon^j_n = \sqrt{(\xi^j_n)^2 + (\Delta^j)^2}$, with ξ^j_n and Δ^j being the single-particle energy level n in the normal state of lead j, and the gap parameter in that lead, respectively. The occupations of the quasiparticle states are described by the distribution functions

$$f^j(\xi^j_n) = \langle\!\langle \hat{\alpha}^{j\dagger}_{n\uparrow}\hat{\alpha}^j_{n\uparrow}\rangle\!\rangle_{\rm qp} = \langle\!\langle \hat{\alpha}^{j\dagger}_{n\downarrow}\hat{\alpha}^j_{n\downarrow}\rangle\!\rangle_{\rm qp}\,, \quad j = L, R\,, \quad (4)$$

assumed to be independent of spin; double angular brackets $\langle\!\langle \ldots\rangle\!\rangle_{\rm qp}$ denote averaging over the quasiparticle states. Hereinafter we assume for simplicity equal gaps in the leads, $\Delta^L = \Delta^R \equiv \Delta$.

The last term in Eq. (1) describes quasiparticle tunneling across the junction and couples the phase and quasiparticle degrees of freedom

$$\hat{H}_T = \tilde{t}\sum_{n,m,\sigma}\left(e^{i\frac{\hat{\varphi}}{2}}u^L_n u^R_m - e^{-i\frac{\hat{\varphi}}{2}}v^R_m v^L_n\right)\hat{\alpha}^{L\dagger}_{n\sigma}\hat{\alpha}^R_{m\sigma} + \text{H.c.} \quad (5)$$

The electron tunneling amplitude t in this equation determines the junction conductance, $g_T = 4\pi e^2\nu^L\nu^R\tilde{t}^2$ in the tunneling limit $\tilde{t} \ll 1$ which we are considering. From now on, we assume identical densities of states per spin direction in the leads, $\nu^L = \nu^R = \nu_0$. The Bogoliubov amplitudes u^j_n, v^j_n can be taken real, since Eq. (5) already accounts explicitly for the phases of the order parameters in the leads via the gauge-invariant phase difference[11] in the exponentials. Accounting for the Josephson effect and quasiparticles dynamics by Eqs. (2)-(5) is possible as long as the qubit energy ω and characteristic energy

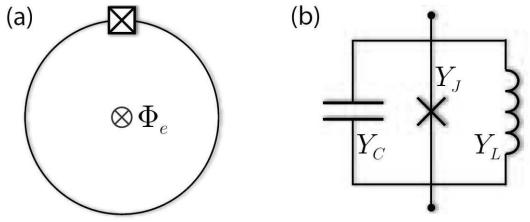

FIG. 1: (a) Schematic representation of a qubit controlled by a magnetic flux, see Eq. (2). (b) Effective circuit diagram with three parallel elements – capacitor, Josephson junction, and inductor – characterized by their respective admittances.

δE of quasiparticles (as determined by their distribution function and measured from Δ) are small compared to Δ:[5] $\omega, \delta E \ll 2\Delta$. In this low-energy limit, we may further approximate $u^j_m \simeq v^j_n \simeq 1/\sqrt{2}$. Then the operators $e^{\pm i\hat{\varphi}/2}$ in Eq. (5), which describe transfer of charge $\pm e$ across the junction, combine to give

$$\hat{H}_T = \tilde{t}\sum_{n,m,\sigma} i\sin\frac{\hat{\varphi}}{2}\hat{\alpha}^{L\dagger}_{n\sigma}\hat{\alpha}^R_{m\sigma} + \text{H.c.} \qquad (6)$$

Starting from this low-energy tunneling Hamiltonian, in the next section we calculate the dissipative part of the junction admittance.

A. Response to a classical time-dependent phase

We consider here the "classical" dissipative response of a Josephson junction to a small ac bias to show that Eq. (6) correctly accounts for the known[11] junction losses in the low-energy regime. These "classical" losses are directly related to the decay rate in the quantum regime, as we explicitly show in the next section.

We assume a time-dependent bias $v(t) = v\cos(\omega t)$ of frequency $\omega > 0$ superimposed to a fixed phase difference φ_0. In other words, we take the phase to be a time-dependent number which, by the Josephson equation $d\varphi/dt = 2ev(t)$, has the form

$$\varphi(t) = \varphi_0 + \frac{2ev}{\omega}\sin(\omega t)\,. \qquad (7)$$

Here we focus on the linear in v response in the low-energy regime. Expressions for the current through the junction valid beyond linear response can be found, for example, in Ref. 11. Substituting Eq. (7) into Eq. (6), expanding for small v, and keeping the linear term, we find for the time-dependent perturbation $\delta\hat{H}(t)$ causing the dissipation

$$\begin{aligned}\delta\hat{H}(t) &= \hat{H}_{AC}\sin(\omega t)\,,\\ \hat{H}_{AC} &= i\tilde{t}\cos\frac{\varphi_0}{2}\frac{ev}{\omega}\sum_{n,m,\sigma}\hat{\alpha}^{L\dagger}_{n\sigma}\hat{\alpha}^R_{m\sigma} + \text{H.c.}\end{aligned} \qquad (8)$$

The average dissipated power can be calculated using Fermi's golden rule: it is given by the product of the transition rate times the energy change in a transition between quasiparticle states caused by the perturbation. The energy change in a transition is $\pm\omega$ by energy conservation, with the two signs corresponds to the events giving energy to or taking energy from the system. The average power P is

$$\begin{aligned}P = 2\pi\sum_{\{\lambda\}_{\rm qp}}\langle\!\langle\left|\langle\{\lambda\}_{\rm qp}|\hat{H}_{AC}|\{\eta\}_{\rm qp}\rangle\right|^2\omega\\ \times[\delta(E_{\lambda,\rm qp} - E_{\eta,\rm qp} - \omega) - \delta(E_{\lambda,\rm qp} - E_{\eta,\rm qp} + \omega)]\rangle\!\rangle_{\rm qp}\,,\end{aligned} \qquad (9)$$

where $E_{\eta,\rm qp}$ and $E_{\lambda,\rm qp}$ are the total energies of the quasiparticles in their respective initial $\{\eta\}_{\rm qp}$ and final $\{\lambda\}_{\rm qp}$

states. We use Eq. (8) to evaluate the matrix element, average over initial quasiparticle states, and sum over final states to find

$$P = \frac{1}{2}\mathrm{Re}\, Y_J(\omega,\varphi_0)v^2 \tag{10}$$

with[12]

$$\mathrm{Re}\, Y_J(\omega,\varphi) = \frac{1+\cos\varphi}{2}\mathrm{Re}\, Y_{\rm qp}(\omega). \tag{11}$$

Here $\mathrm{Re}\, Y_{\rm qp}$ is the real part of the quasiparticle contribution to the junction admittance at zero phase difference,

$$\mathrm{Re}\, Y_{\rm qp}(\omega) = g_T\frac{2\Delta}{\omega}\int_0^\infty dx\,\frac{1}{\sqrt{x}\sqrt{x+\omega/\Delta}} \left[f_E\left((1+x)\Delta\right) - f_E\left((1+x+\omega/\Delta)\Delta\right)\right]. \tag{12}$$

In deriving these formulas we have approximated the standard BCS density of states functions as

$$\frac{\epsilon}{\sqrt{\epsilon^2-\Delta^2}},\ \frac{\Delta}{\sqrt{\epsilon^2-\Delta^2}} \sim \sqrt{\frac{\Delta}{2(\epsilon-\Delta)}} \equiv \frac{1}{\sqrt{2x}} \tag{13}$$

and taken equal quasiparticle occupations in the two leads, $f^L = f^R \equiv f$; we use this simplifying assumption throughout the paper. We indicate with f_E the energy mode of the distribution function

$$f_E(\epsilon) = \frac{1}{2}\left[f(\xi) + f(-\xi)\right], \tag{14}$$

where $\epsilon = \sqrt{\xi^2+\Delta^2}$. Equation (11) for the real part of the admittance, valid at $\omega > 0$, agrees with the linear response, low-energy limit of the non-linear I-V characteristic presented in Ref. 11. Extension to $\omega < 0$ is found by noticing that $\mathrm{Re}\, Y_{\rm qp}$ is an even function of frequency.

In thermal equilibrium and at low temperatures $T \ll \Delta$ the distribution function can be approximated as

$$f_E(\epsilon) \simeq e^{-\epsilon/T}, \tag{15}$$

and Eq. (12) gives, at arbitrary ratio ω/T,

$$\mathrm{Re}\, Y^{eq}_{\rm qp}(\omega) = g_T\frac{2\Delta}{\omega}e^{-\Delta/T}e^{\omega/2T}K_0\left(\frac{|\omega|}{2T}\right)\left[1-e^{-\omega/T}\right]. \tag{16}$$

Here K_0 is the modified Bessel function of the second kind with asymptotes

$$K_0(x) \simeq \begin{cases} e^{-x}\sqrt{\pi/2x}\,, & x \gg 1 \\ \ln 2/x - \gamma_E\,, & x \ll 1 \end{cases} \tag{17}$$

with γ_E the Euler gamma.

For a generic distribution function, we can relate $\mathrm{Re}\, Y_{\rm qp}$ to the density of quasiparticle $n_{\rm qp}$ in the high-frequency regime $\omega \gg \delta E$, where δE indicates the characteristic energy of quasiparticle (measured from the gap) above which the occupation of the quasiparticle states can be neglected; in thermal equilibrium $\delta E \sim T$. Under the assumption $\omega \gg \delta E$ we obtain from Eq. (12)

$$\mathrm{Re}\, Y^{hf}_{\rm qp}(\omega) = \frac{1}{2}x_{\rm qp}\, g_T\left(\frac{2\Delta}{|\omega|}\right)^{3/2}, \tag{18}$$

where

$$x_{\rm qp} = \frac{n_{\rm qp}}{2\nu_0\Delta} \tag{19}$$

is the quasiparticle density normalized to the Cooper pair density and

$$n_{\rm qp} = 2\sqrt{2}\nu_0\Delta\int_0^\infty \frac{dx}{\sqrt{x}}f_E((1+x)\Delta) \tag{20}$$

is the density written using the approximation in Eq. (13). Note that in thermal equilibrium at low temperatures, Eq. (15), we have

$$n^{eq}_{\rm qp} = 2\nu_0\sqrt{2\pi\Delta T}e^{-\Delta/T}. \tag{21}$$

Then using Eq. (17), it is easy to check that for $T \ll \omega$ Eq. (16) takes the form given in Eq. (18).

The real and imaginary parts of the admittance satisfy the Kramers-Krönig relations. However, when taking the Kramers-Krönig transform of the real part, a purely inductive contribution to the imaginary part can be missed. Indeed, at low energies the complex junction admittance (obtained from the expressions in Ref. 11) can be written as

$$Y_J(\omega,\varphi) = \frac{1-2x^{\rm A}_{\rm qp}}{i\omega L_J}\cos\varphi + Y_{\rm qp}(\omega)\frac{1+\cos\varphi}{2}, \tag{22}$$

where

$$x^{\rm A}_{\rm qp} = f_E(\Delta) \tag{23}$$

can be interpreted as the population of the Andreev bound states[13] and the inverse of the Josephson inductance is

$$\frac{1}{L_J} = g_T\pi\Delta_{\rm qp} \tag{24}$$

(the subscript qp in $\Delta_{\rm qp}$ is used to indicate that in this expression it may be necessary to account for the effect of quasiparticles on the gap, see Secs. II C and III B).

Unlike the Andreev states, free quasiparticles contribute to both dissipative and non-dissipative parts of the total admittance Y_J via the complex term $Y_{\rm qp}$. The real part of the quasiparticle admittance is defined in Eq. (12), while its imaginary part is given by the Kramers-Krönig transform of that expression,

$$\mathrm{Im}\, Y_{\rm qp}(\omega) = -g_T\frac{2\Delta}{\omega}\frac{P}{\pi}\int_0^\infty\frac{dx}{\sqrt{x}}\int_0^\infty\frac{dy}{\sqrt{y}}\Big[f_E\left((1+x)\Delta\right) - f_E\left((1+y)\Delta\right)\Big]\left[\frac{1}{x-y+\omega/\Delta} - \frac{1}{x-y}\right], \tag{25}$$

where P denotes the principal part and $\omega > 0$. Using that $\mathrm{Im}\, Y_{\rm qp}$ is an odd function of frequency, we can simplify the above expression to a form with a single rather than double integral

$$\mathrm{Im}\, Y_{\rm qp}(\omega) = g_T \frac{2\Delta}{\omega}\left[\int_0^{|\omega|/\Delta} dx\, \frac{f_E\left((1+x)\Delta\right)}{\sqrt{x}\sqrt{|\omega|/\Delta - x}} - \pi x_{\rm qp}^{\rm A}\right]. \tag{26}$$

As discussed above for the real part, an analytic expression for $\mathrm{Im}\, Y_{\rm qp}$ can be obtained in thermal equilibrium,

$$\mathrm{Im}\, Y_{\rm qp}^{eq}(\omega) = -g_T \frac{2\Delta}{\omega} e^{-\Delta/T}\pi\left[1 - e^{-|\omega|/2T} I_0\left(\frac{|\omega|}{2T}\right)\right]. \tag{27}$$

Here I_0 is the modified Bessel function of the first kind with asymptotes

$$I_0(x) \simeq \begin{cases} e^x\sqrt{1/2\pi x}\,, & x \gg 1 \\ 1 + x^2/4\,, & x \ll 1 \end{cases}. \tag{28}$$

For arbitrary distribution function satisfying the high-frequency condition $\omega \gg \delta E$ we find

$$\mathrm{Im}\, Y_{\rm qp}^{hf}(\omega) = \frac{1}{2} g_T \frac{2\Delta}{\omega}\left[x_{\rm qp}\sqrt{\frac{2\Delta}{|\omega|}} - 2\pi x_{\rm qp}^{\rm A}\right]. \tag{29}$$

Using Eq. (21) and the large-x limit in Eq. (28), it is easy to show that for $T \ll \omega$ Eq. (27) reduces to the general expression in Eq. (29). In the high-frequency regime, real and imaginary parts of the quasiparticle admittance can be combined into the complex admittance

$$Y_{\rm qp}^{hf}(\omega) = -\frac{2}{i\omega L_J}\left[\frac{x_{\rm qp}}{\pi}\sqrt{\frac{\Delta}{i\omega}} - x_{\rm qp}^{\rm A}\right]. \tag{30}$$

By substituting Eq. (30) into Eq. (22) we find that in the total admittance Y_J the coefficient multiplying $x_{\rm qp}^{\rm A}$ is proportional to $(1-\cos\varphi)$ and vanishes for $\varphi = 0$. This is in agreement with the absence of Andreev bound states when there is no phase difference across the junction.

B. Transition rates

The effects of the interaction between quasiparticles and qubit degree of freedom, Eq. (5), can be treated perturbatively in the tunneling amplitude $\tilde{t}$. The interaction makes possible, for example, a transition between two qubit states (initial, $|i\rangle$, and final, $|f\rangle$, differing in energy by amount $\omega_{if} > 0$) by exciting a quasiparticle during a tunneling event. The rate for the transition between qubit states can be calculated using Fermi's golden rule

$$\Gamma_{i\to f} = 2\pi \sum_{\{\lambda\}_{\rm qp}} \langle\!\langle \left|\langle f, \{\lambda\}_{\rm qp}|\hat{H}_T|i, \{\eta\}_{\rm qp}\rangle\right|^2 \times \delta\left(E_{\lambda,\rm qp} - E_{\eta,\rm qp} - \omega_{if}\right)\rangle\!\rangle_{\rm qp}\,. \tag{31}$$

We remind that in our notation $E_{\eta,\rm qp}$ ($E_{\lambda,\rm qp}$) is the total energy of the quasiparticles in their initial (final) state $\{\eta\}_{\rm qp}$ ($\{\lambda\}_{\rm qp}$), and double angular brackets $\langle\!\langle \ldots \rangle\!\rangle_{\rm qp}$ denote averaging over the initial quasiparticle states whose occupation is determined by the distribution function.

In the low-energy regime we are considering, the transition rate factorizes into terms accounting separately for qubit dynamic and quasiparticle kinetics

$$\Gamma_{i\to f} = \left|\langle f|\sin\frac{\hat{\varphi}}{2}|i\rangle\right|^2 S_{\rm qp}\left(\omega_{if}\right). \tag{32}$$

Equation (32) is one of the main results of this work: it shows that the qubit properties affect the transition rate via the wavefunctions $|i\rangle$, and $|f\rangle$ entering the matrix element, while the quasiparticle kinetics is accounted for by the quasiparticle current spectral density $S_{\rm qp}$

$$S_{\rm qp}\left(\omega\right) = \frac{16E_J}{\pi}\int_0^\infty dx\, \frac{1}{\sqrt{x}\sqrt{x+\omega/\Delta}}\Big[f_E\left((1+x)\Delta\right) \times\left(1 - f_E\left((1+x)\Delta + \omega\right)\right)\Big], \tag{33}$$

where $\omega > 0$ and we used the relation

$$E_J = g_T\Delta/8g_K \tag{34}$$

with $g_K = e^2/2\pi$ the conductance quantum. The expression for $S_{\rm qp}$ at $\omega < 0$ is obtained by the replacements $x \to x - \omega/\Delta$, $\omega \to -\omega$ in the integrand in Eq. (33).

The spectral density $S_{\rm qp}$ depends on the detail of the distribution functions. In thermal equilibrium at low temperatures $T \ll \Delta$, using Eq. (15) we find

$$S_{\rm qp}^{eq}(\omega) = \frac{16E_J}{\pi} e^{-\Delta/T} e^{\omega/2T} K_0\left(\frac{|\omega|}{2T}\right). \tag{35}$$

Note that the equality

$$\frac{S_{\rm qp}^{eq}(-\omega)}{S_{\rm qp}^{eq}(\omega)} = e^{-\omega/T} \tag{36}$$

implies that in thermal equilibrium the transition rates are related by detailed balance,

$$\frac{\Gamma_{f\to i}}{\Gamma_{i\to f}} = e^{-\omega_{if}/T}. \tag{37}$$

The similarity between Eq. (35) for $S_{\rm qp}$ and Eq. (16) for $\mathrm{Re}\, Y_{\rm qp}$ is not accidental. In thermal equilibrium the following fluctuation-dissipation relation holds

$$S_{\rm qp}^{eq}(\omega) + S_{\rm qp}^{eq}(-\omega) = \frac{\omega}{\pi}\frac{1}{g_K}\mathrm{Re}\, Y_{\rm qp}^{eq}(\omega)\coth\left(\frac{\omega}{2T}\right). \tag{38}$$

Moreover, in the low-energy regime for an *arbitrary* distribution function the two quantities are also related by

$$S_{\rm qp}(\omega) - S_{\rm qp}(-\omega) = \frac{\omega}{\pi}\frac{1}{g_K}\mathrm{Re}\, Y_{\rm qp}(\omega)\,. \tag{39}$$

In the high-frequency regime $\omega \gg \delta E$, we can simplify the above relation to

$$S^{hf}_{\rm qp}(\omega) = \frac{\omega}{\pi}\frac{1}{g_K}{\rm Re}\, Y^{hf}_{\rm qp}(\omega). \tag{40}$$

For the transition rates this corresponds to neglecting the downward transitions with $\omega_{if} < 0$, in which a quasiparticle looses energy to the qubit, compared to the upward ones. This is a good approximation since the assumption $\omega \gg \delta E$ means that there are no quasiparticles with energy high enough to excite the qubit. Equation (40) can be checked by comparing Eq. (18) to

$$S^{hf}_{\rm qp}(\omega) = x_{\rm qp}\frac{8E_J}{\pi}\sqrt{\frac{2\Delta}{\omega}} \tag{41}$$

with E_J given in Eq. (34) and the the normalized quasiparticle density $x_{\rm qp}$ in Eq. (19).

C. Energy level corrections

In addition to causing transitions between qubit levels, the quasiparticles affect the energy E_i of each level i of the system. We can distinguish two quasiparticle mechanisms that modify the qubit spectrum and hence separate two terms in the correction δE_i to the energy,

$$\delta E_i = \delta E_{i,E_J} + \delta E_{i,{\rm qp}}\,. \tag{42}$$

First, in the presence of quasiparticles the Josephson energy takes the form

$$E_{J,{\rm qp}} = \frac{g_T}{8g_K}\Delta_{\rm qp}(1-2x^{\rm A}_{\rm qp}) \tag{43}$$

with $x^{\rm A}_{\rm qp}$ defined in Eq. (23). As mentioned after Eq. (24), we use $\Delta_{\rm qp}$ to distinguish the self-consistent gap in the presence of quasiparticles from the gap Δ when there are no quasiparticles. At leading order in the quasiparticle density we have

$$\Delta_{\rm qp} \simeq \Delta\,(1-x_{\rm qp})\,. \tag{44}$$

Treating these modifications to the Josephson energy as perturbations, the correction to the energy of level i is

$$\delta E_{i,E_J} = E_J\left(x_{\rm qp} + 2x^{\rm A}_{\rm qp}\right)\langle i|\cos\hat\varphi|i\rangle\,. \tag{45}$$

Second, the virtual transitions between the qubit levels mediated by quasiparticle tunneling cause a correction that can be expressed in terms of the matrix elements of $\sin\hat\varphi/2$ as

$$\delta E_{i,{\rm qp}} = \sum_{k\neq i}\left|\langle k|\sin\frac{\hat\varphi}{2}|i\rangle\right|^2 F_{\rm qp}\left(\omega_{ik}\right)\,, \tag{46}$$

where

$$\omega_{ik} = E_k - E_i\,. \tag{47}$$

The derivation of the above formulas and the definition of function $F_{\rm qp}$ in terms of the quasiparticle distribution function [Eq. (A19)] are given in Appendix A. Here we give the relation between $F_{\rm qp}$ and the imaginary part of the quasiparticle impedance,

$$F_{\rm qp}(\omega) + F_{\rm qp}(-\omega) = -\frac{\omega}{2\pi}\frac{1}{g_K}{\rm Im}\, Y_{\rm qp}(\omega), \tag{48}$$

which we will use in the next section to obtain the quasiparticle-induced change in the qubit frequency.

III. SINGLE JUNCTION: WEAKLY ANHARMONIC QUBIT

As an application of the general approach described in the previous section, we consider here a weakly anharmonic qubit, such as the transmon and phase qubits. We start with the the semiclassical limit, i.e., we assume that the potential energy terms in Eq. (2) dominate the kinetic energy term proportional to E_C. This limit already reveals a non-trivial dependence of relaxation on flux. Note that assuming $E_L \neq 0$ we can eliminate n_g in Eq. (2) by a gauge transformation.[14] In the transmon we have $E_L = 0$ and the spectrum depends on n_g, displaying both well separated and nearly degenerate states, see Fig. 2. The results of this section can be applied to the single-junction transmon when considering well separated states. The transition rate between these states and the corresponding frequency shift are dependent on n_g. However, since $E_C \ll E_J$ this dependence introduces only small corrections to $\Gamma_{n\to n-1}$ and $\delta\omega$; the corrections are exponential in $-\sqrt{8E_J/E_C}$. By contrast, the leading term in the rate of transitions $\Gamma_{e\leftrightarrow o}$ between the even and odd states is exponentially small. The rate $\Gamma_{e\leftrightarrow o}$ of parity switching is discussed in detail in Appendix C.

The potential energy in Eq. (2) is extremized at phase φ_0 satisfying

$$E_J\sin\varphi_0 + E_L\left(\varphi_0 - 2\pi\Phi_e/\Phi_0\right) = 0. \tag{49}$$

For $E_J < E_L$ there is only one solution at the global minimum. For $E_J > E_L$ however, there can be multiple minima; their number depends both on the ratio E_J/E_L and the external flux Φ_e. Here we assume that the flux is such that distinct minima are not degenerate; in particular, this means that the flux is tuned away from odd integer multiples of half the flux quantum.[15] For the transmon with $E_L = 0$, we can take $\varphi_0 = 0$ as solution to Eq. (49). Next, we expand the potential energy around a minimum and find at quadratic order

$$\hat H^{(2)}_\varphi = 4E_C\hat n^2 + \frac{1}{2}\left(E_L + E_J\cos\varphi_0\right)\left(\hat\varphi - \varphi_0\right)^2. \tag{50}$$

Fluctuations of the phase around φ_0 are small under the assumption

$$n\frac{E_C}{\omega_{10}} \ll 1, \tag{51}$$

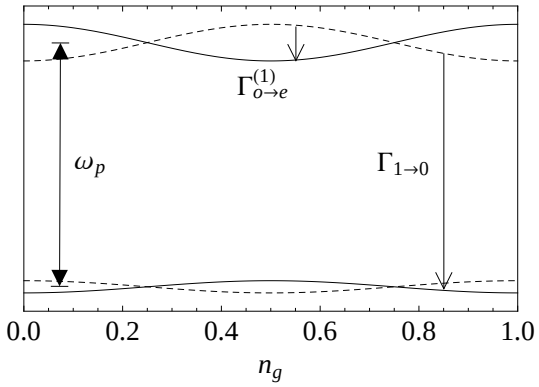

FIG. 2: Schematic representation of the transmon low energy spectrum as function of the dimensionless gate voltage n_g. Solid (dashed) lines denotes even (odd) states (see also Sec. IV A). The amplitudes of the oscillations of the energy levels are exponentially small,[2] see Appendix B; here they are enhanced for clarity. Quasiparticle tunneling changes the parity of the qubit sate. The results of Sec. III are valid for transitions between states separated by energy of the order of the plasma frequency ω_p, Eq. (56), and give, for example, the rate $\Gamma_{1\to0}$. For the transition rates between nearly degenerate states of opposite parity, such as $\Gamma^{(1)}_{o\to e}$, see Appendix C.

where n denotes the energy level and

$$\omega_{10} = \sqrt{8E_C\left(E_L + E_J\cos\varphi_0\right)} \tag{52}$$

is the qubit frequency in the harmonic approximation. Note that anharmonicity and quality factor Q determine the operability of the system as a qubit.[8] The anharmonic correction to the transition frequencies can be calculated by considering the effect on the spectrum of the next order in the expansion around φ_0 (cubic for the phase qubit, quartic for the transmon), which defines an anharmonic potential well of finite depth U. Then the operability condition can be expressed as $Q/n_w \gg 1$, where n_w is the number of states in the potential well, $n_w \sim U/\omega_{10}$.[16] In a weakly anharmonic system, n_w can be large; however, if the quality factor is larger the system can be used as a qubit despite the weak anharmonicity, as it is indeed the case for the transmon.[2]

The condition for small phase fluctuations in Eq. (51) enables us to calculate the matrix element of operator $\sin\hat{\varphi}/2$ by expanding around φ_0 up to the second order and using standard expressions for the matrix elements of the position operator between eigenstates $|n\rangle$, $|m\rangle$ of the harmonic oscillator [cf. Eq. (50)]. To first order in E_C/ω_{10} we find (see also Appendix D)

$$\left|\langle m|\sin\frac{\hat{\varphi}}{2}|n\rangle\right|^2 = \delta_{m,n}\left[1-2\frac{E_C}{\omega_{10}}\left(n+\frac{1}{2}\right)\right]\frac{1-\cos\varphi_0}{2} + \frac{E_C}{\omega_{10}}\left[n\delta_{m,n-1}+(n+1)\,\delta_{m,n+1}\right]\frac{1+\cos\varphi_0}{2}\,. \tag{53}$$

Note that in the first term on the right hand side the corrections due to the non-linearity of sine (the second term inside the square brackets) are indeed small if condition (51) is satisfied. In addition, we have neglected here the anharmonic corrections to the states used to calculate the matrix element; this is a good approximation for low-lying levels $n \ll n_w$.[17] For the transmon ($\varphi_0 = 0$) the leading term in Eq. (53) is of linear order in $E_C/\omega_{10} \ll 1$; as we show in Appendix E by including the first anharmonic correction to the states, the next non-vanishing term in the square of the transmon matrix element is cubic in E_C/ω_{10}, rather than quadratic as for the harmonic oscillator. Therefore in the case of the transmon keeping only the leading term is a better approximation than naively expected.

Equation (53) shows that at leading order we can restrict our attention to transitions involving only neighboring levels. Concentrating here on low-lying levels, using Eqs. (32), (39), and (53) we find the following relation between transition rate and impedance

$$\Gamma_{n\to n-1} - \Gamma_{n-1\to n} = \frac{n}{C}\mathrm{Re}\,Y_{\rm qp}(\omega_{10})\frac{1+\cos\varphi_0}{2}, \tag{54}$$

where we also used $E_C = e^2/2C$. In the high-frequency regime, the upward transition rate can be neglected, $\Gamma_{n-1\to n} \simeq 0$, and the above expression simplifies to[19] [see also Eq. (40) and the text that follows it]

$$\begin{aligned}\Gamma_{n\to n-1} &= \frac{n}{C}\mathrm{Re}\,Y^{hf}_{\rm qp}(\omega_{10})\frac{1+\cos\varphi_0}{2}\\ &= n\frac{\omega_p^2}{\omega_{10}}\frac{x_{\rm qp}}{2\pi}\sqrt{\frac{2\Delta}{\omega_{10}}}\left(1+\cos\varphi_0\right)\,.\end{aligned} \tag{55}$$

In the last expression we used Eq. (18) and introduced the plasma frequency

$$\omega_p = \sqrt{8E_CE_J}\,. \tag{56}$$

The above equation can also be obtained by substituting directly Eq. (40) into Eq. (32). For $n = 1$ and $\varphi_0 = 0$ Eq. (55) reduces to the transition rate presented in Ref. 3.

The transition rate in Eq. (55) is proportional to the (possibly non-equilibrium) quasiparticle density $x_{\rm qp}$ and depends on the external flux Φ_e via φ_0 and ω_{10}, see Eqs. (49) and (52). The flux dependence is in general sensitive to the states involved in the transition. This sensitivity can already be seen for transitions between harmonic oscillator states: due to the non-linear interaction between phase and quasiparticles, see Eq. (6), transitions between distant levels are possible. These transitions are suppressed by the smallness of phase fluctuations when $E_C/\omega_{10} \ll 1$. For example, the rate for the $2 \to 0$ transition is

$$\Gamma_{2\to0} = \frac{2\omega_{10}}{\pi}\frac{1}{g_K}\mathrm{Re}\,Y^{hf}_{\rm qp}(2\omega_{10})\left(\frac{E_C}{\omega_{10}}\right)^2\frac{1-\cos\varphi_0}{4}. \tag{57}$$

Note that in contrast to Eq. (55), Eq. (57) cannot be written in terms of the real part of the total admittance of the junction: while in Eq. (55) the phase enters via

the factor $(1+\cos\varphi_0)$ as in Eq. (11), in Eq. (57) $\mathrm{Re}\, Y_{\rm qp}$ is multiplied by $(1-\cos\varphi_0)$. To obtain $\Gamma_{2\to0}$ we substituted into Eq. (32) the high-frequency relation (40), while the explicit form of the squared matrix element $|\langle 0|\sin(\hat\varphi/2)|2\rangle|^2$ is found by setting $n=2$, and keeping the leading term in E_C/ω_{10}, in the formula

$$\left|\langle 0|\sin\frac{\hat\varphi}{2}|n\rangle\right|^2 = e^{-\frac{E_C}{\omega_{10}}}\left(\frac{E_C}{\omega_{10}}\right)^n \frac{1-(-1)^n\cos\varphi_0}{2n!} \quad (58)$$

derived in Appendix D. Equation (58) is valid for any ratio E_C/ω_{10} for transitions between eigenstates of the harmonic oscillator. When $\varphi_0=0$, Eq. (58) gives vanishing matrix elements for even n – this is an example of the more general selection rule according to which only transitions between states of different parity are allowed at $\varphi_0=0$.

The rate for transitions between excited states and the ground state in the case of large phase fluctuations can be obtained using Eq. (58) when $E_L \ll E_C$ and $E_J \lesssim \omega_{LC}=\sqrt{8E_CE_L}$. The latter condition enables us to neglect the Josephson energy term in Eq. (2). Then using Eqs. (32) and (41) with $\omega_{if}=n\omega_{LC}$ we find that the transition rate has a maximum for $n=n_0$ with $n_0\approx E_C/\omega_{LC}$,

$$\Gamma_{n\to0}\simeq\frac{\omega_p^2}{E_C}\frac{x_{\rm qp}}{2\pi}\sqrt{\frac{2\Delta}{E_C}}\left[1-(-1)^n\cos 2\pi\Phi_e/\Phi_0\right] \times\frac{1}{\sqrt{2\pi n_0}}\exp\left[-\frac{(n-n_0)^2}{2n_0}\right]. \quad (59)$$

Here we have approximated $e^{-y}y^n/n!\sqrt{n}\simeq\exp[-(n-y)^2/2y]/\sqrt{2\pi}\,y$; the approximation is valid for $y\gg1$ and $|n-y|\lesssim\sqrt{2y}$. Equation (59) shows that when the charging energy is the dominant energy scale, dissipation is the strongest for transitions between states whose energy difference ($n\omega_{LC}$) corresponds to the energy change (E_C) caused by the transfer of a single electron through the barrier, as in the "quasiparticle poisoning" picture for the Cooper pair box.[5] We stress that in the present case charge is not quantized, due to the finite value of the inductive energy E_L.[14] We will comment on the relation between Eq. (59) and the transition rate in the Cooper pair box in Sec. IV A.

A. Quality factor

Returning now to the semiclassical regime of small E_C, Eq. (55) with $n=1$ enables us to evaluate, in the high-frequency regime, the inverse Q-factor for the transition between the qubit states

$$\frac{1}{Q_{10}}=\frac{\Gamma_{1\to0}}{\omega_{10}}=\frac{1}{\pi g_K}\mathrm{Re}\, Y_{\rm qp}^{hf}(\omega_{10})\frac{E_C}{\omega_{10}}\frac{1+\cos\varphi_0}{2}. \quad (60)$$

We stress that this formula is valid not only in thermal equilibrium, but also in the presence of non-equilibrium quasiparticles with characteristic energy $\delta E\ll\omega_{10}$. We can generalize Eq. (60) to account for the possible coexistence of non-equilibrium and thermal quasiparticles. We take the distribution function in the form

$$f_E(\epsilon)=f_{ne}(\epsilon)+f_{eq}(\epsilon), \quad (61)$$

where f_{ne} is the non-equilibrium contribution, insensitive to temperature and satisfying the high-frequency condition $\omega_{10}\gg\delta E$, and f_{eq} is the equilibrium distribution of Eq. (15). Noting that within our assumption the two terms in f_E contribute separately to the transition rates and that for the thermal part we cannot in general neglect the "upward" transitions, using Eqs. (32), (35), (41), and (53) we find

$$\frac{1}{Q_{10}}=\frac{\Gamma_{1\to0}+\Gamma_{0\to1}}{\omega_{10}}=\frac{1+\cos\varphi_0}{2\pi}\frac{\omega_p^2}{\omega_{10}^2}\left[x_{ne}\sqrt{\frac{2\Delta}{\omega_{10}}} +4e^{-\Delta/T}\cosh\left(\frac{\omega_{10}}{2T}\right)K_0\left(\frac{\omega_{10}}{2T}\right)\right], \quad (62)$$

where x_{ne} is the normalized non-equilibrium quasiparticle density [cf. Eq. (19)].

Recently good agreement between theory, Eq. (62), and experiment has been shown for single-junction transmons ($\varphi_0=0$, $\omega_{10}=\omega_p$) in the temperature range 10-210 mK.[20] However, while these measurements indicate that thermal quasiparticles are the main cause of relaxation above $\sim$ 150 mK, one cannot conclude that non-equilibrium quasiparticles are present from the lower temperature data: by Matthiessen rule, any other relaxation mechanism which is independent of (or weakly dependent on) temperature would have the same limiting effect on Q_{10} as the first term in square brackets in Eq. (62). As we will discuss in more detail in Sec. V A, similar measurements on a flux-sensitive device should enable one to decide on the presence of non-equilibrium quasiparticles, since Eq. (62) [and its analogous for the split transmon, Eq. (127)] describes the effect of flux on both equilibrium and non-equilibrium quasiparticle contributions to Q_{10}, and other sources of relaxation respond differently to the flux.

B. Frequency shift

A further test of the theory presented in Sec. II is provided by the measurement of the qubit resonant frequency. In the semiclassical regime of small E_C, the qubit can be described by the effective circuit of Fig. 1(b), with the junction admittance Y_J of Eq. (22), $Y_C=i\omega C$, and $Y_L=1/i\omega L$ [the inductance is related to the inductive energy by $E_L=(\Phi_0/2\pi)^2/L$]. As discussed in Ref. 10, for parallel elements the total admittance Y is the sum of their admittances,

$$Y=Y_J+Y_C+Y_L, \quad (63)$$

and the resonant frequency ω_r is the zero of the total admittance, $Y(\omega_r)=0$. In the absence of quasiparticles we find $\omega_r=\omega_{10}$ with ω_{10} of Eq. (52).

In the presence of quasiparticles, by considering their effect on the junction admittance at linear order in the quasiparticle density $x_{\rm qp}$ and Andreev level occupation $x_{\rm qp}^{\rm A}$ we obtain

$$\omega_r = \omega_{10} + \delta\omega \tag{64}$$

with

$$\begin{aligned}\delta\omega = \frac{i}{2C}Y_{\rm qp}(\omega_{10})\frac{1+\cos\varphi_0}{2} - \frac{\pi g_T\Delta}{C\omega_{10}}x_{\rm qp}^{\rm A}\cos\varphi_0 \\ -\frac{\pi g_T\Delta}{2C\omega_{10}}x_{\rm qp}\cos\varphi_0\,.\end{aligned} \tag{65}$$

The last term in Eq. (65) originates from the gap suppression by quasiparticles [cf. Eq. (44)]. This term was neglected in Ref. 10 as it is subleading in the high-frequency regime considered there [see Eq. (73)]. The correction $\delta\omega$ has both real and imaginary parts. The imaginary part coincides[10] with half the dissipation rate in Eq. (55) for the $n = 1 \to 0$ transition. Here we show that the real part of $\delta\omega_r$ obtained in the effective circuit approach agrees with the quantum mechanical calculation.

Within the harmonic approximation of Eq. (50), the energy difference ω_i between the neighboring levels E_{i+1} and E_i,

$$\omega_i \equiv E_{i+1} - E_i = \omega_{10}\,, \tag{66}$$

is of course independent of the level index i. The quasiparticle corrections to energy levels of Sec. II C cause a correction $\delta\omega_i$ to ω_i,

$$\delta\omega_i = \delta E_{i+1} - \delta E_i\,. \tag{67}$$

As we show below, at leading order in E_C/ω_{10} this correction is also independent of level index, i.e, it represents a renormalization of the system resonant frequency.

As in Eq. (42), we separate the contributions due to change in the Josephson energy and due to quasiparticle tunneling,

$$\delta\omega_i = \delta\omega_{i,E_J} + \delta\omega_{i,\rm qp}. \tag{68}$$

For the first term on the right hand side, we use Eq. (45) together with the matrix element of $\cos\hat\varphi$ at first order in E_C/ω_{10} [see Eq. (D9)],

$$\langle i|\cos\hat\varphi|i\rangle \simeq \cos\varphi_0\left[1 - \frac{4E_C}{\omega_{10}}\left(i+\frac{1}{2}\right)\right], \tag{69}$$

to find

$$\delta\omega_{i,E_J} = -\frac{1}{2}\frac{\omega_p^2}{\omega_{10}}\cos\varphi_0\left(x_{\rm qp} + 2x_{\rm qp}^{\rm A}\right)\,. \tag{70}$$

As discussed in Sec. II C, the term proportional to $x_{\rm qp}$ is due to the gap suppression in the presence of quasiparticles, Eq. (44), while $x_{\rm qp}^{\rm A}$ accounts for the occupation of the Andreev bound states.

For the quasiparticle tunneling term, we substitute Eq. (53) into Eq. (46) to get

$$\delta\omega_{i,\rm qp} = \frac{E_C}{\omega_{10}}\left[F_{\rm qp}(\omega_{10}) + F_{\rm qp}(-\omega_{10})\right]\frac{1+\cos\varphi_0}{2}\,. \tag{71}$$

Finally, using the relation (48) and adding the two terms we arrive at

$$\begin{aligned}\delta\omega_i = -\frac{1}{2C}\mathrm{Im}\,Y_{\rm qp}(\omega_{10})\frac{1+\cos\varphi_0}{2} \\ -\frac{1}{2}\frac{\omega_p^2}{\omega_{10}}\cos\varphi_0\left(x_{\rm qp} + 2x_{\rm qp}^{\rm A}\right)\,.\end{aligned} \tag{72}$$

This expression agrees with the real part of Eq. (65). We note that by extending the above consideration to include the next order in E_C/ω_{10}, anharmonic corrections to the spectrum can be calculated. They are dominated by the anharmonicity of the cosine potential in Eq. (2), with quasiparticles contributing negligible additional corrections. For the case of the transmon, the leading anharmonicity can be found in Ref. 2.

In the high-frequency regime, using Eq. (29) the relative frequency shift is

$$\begin{aligned}\frac{\delta\omega_i}{\omega_{10}} =& \frac{1}{2}\frac{\omega_p^2}{\omega_{10}^2}\Bigg[x_{\rm qp}^{\rm A}\left(1-\cos\varphi_0\right) \\ &- x_{\rm qp}\left(\frac{1+\cos\varphi_0}{2\pi}\sqrt{\frac{2\Delta}{\omega_{10}}} + \cos\varphi_0\right)\Bigg].\end{aligned} \tag{73}$$

Note that in the limit $\omega_{10} \ll \Delta$ we can neglect the cosine compared to the term multiplied by square root inside round brackets. However, this cosine term is the appropriate subleading contribution, since the terms neglected in deriving the energy corrections presented in Sec. II C are suppressed by ω_{10}/Δ with respect to the leading contribution.

In recent experiments with single-junction transmons[20] relative shifts of order 10^{-5} have been measured at temperatures ~ 200 mK, in agreement with Eq. (72). Together with the above mentioned measurements of the transition rates in the same devices, this is an additional, independent check of the validity of the present theory in the regime $T \gtrsim 150$ mK. While in the transmon ($\varphi_0 = 0$) there are no Andreev bound states [indeed, in this case their contribution to the frequency shift is absent, see Eq. (73)], in a phase qubit both Andreev levels occupation $x_{\rm qp}^{\rm A}$ and free quasiparticle density $x_{\rm qp}$ affect the frequency. Assuming that the two quantity are proportional, $x_{\rm qp}^{\rm A} \propto x_{\rm qp}$,the ratio between frequency shift, Eq. (73), and transition rate, Eq. (55), in the high frequency regime is independent of the quasiparticle density. The constancy of this ratio has been recently verified by injecting a variable (but unknown) number quasiparticles in a phase qubit.[21]

IV. SINGLE JUNCTION: STRONG ANHARMONICITY

Here we consider the regime, complementary to that of the previous section, of qubits with large anharmonicities. We study first the single junction Cooper pair box (CPB); as for the transmon, it is insensitive to flux, but in contrast to the transmon the CPB properties are strongly affected by the value of the dimensionless gate voltage n_g. Then we analyze a flux qubit, for which the external flux is tuned near half the flux quantum, $\Phi_e \approx \Phi_0/2$.

A. Cooper pair box

The CPB is described by Eq. (2) with $E_L = 0$ and $E_C \gg E_J$. In this limit, it is convenient to rewrite the Hamiltonian in the charge basis as[5]

$$\begin{aligned}\hat{H} = & E_C \sum_q \Big(q - 2n_g\Big)^2 |q\rangle\langle q| \\ & - \frac{1}{2} E_J \sum_q \Big(|q\rangle\langle q+2| + |q+2\rangle\langle q|\Big).\end{aligned} \tag{74}$$

The eigenstates have definite parity (even/odd) and are given by linear combinations of even/odd charge states. The CPB operating point is, without loss of generality, at $n_g = 1/2$. Near this operating point, the CPB is well described by the reduced Hamiltonian

$$H_{CPB} = \begin{pmatrix} E_C(2n_g)^2 & 0 & -E_J/2 \\ 0 & E_C(2n_g-1)^2 & 0 \\ -E_J/2 & 0 & E_C(2n_g-2)^2 \end{pmatrix}. \tag{75}$$

The reduced CPB Hamiltonian has a single odd eigenstate, the $|q=1\rangle$ charge state,

$$|o, 0; n_g\rangle = |1\rangle, \tag{76}$$

with n_g-dependent eigenenergy

$$E_0(n_g) = E_C(2n_g - 1)^2\,, \tag{77}$$

and two even eigenstates, $|e, \pm; n_g\rangle$, with energies

$$E_\pm(n_g) = E_C + E_0(n_g) \pm \frac{1}{2}\omega_{10}(n_g)\,. \tag{78}$$

The qubit frequency depends on the gate voltage as

$$\omega_{10}(n_g) = \sqrt{(4E_C)^2(2n_g-1)^2 + E_J^2}\,. \tag{79}$$

Note that at the operating point we have $\omega_{10}(1/2) = E_J$ and that the frequency rises quickly at a narrow distance from the optimal point, more than doubling for $|n_g - 1/2| \sim E_J/E_C \ll 1$. In terms of the charge states, the two even eigenstates are

$$\begin{aligned}|e, -; n_g\rangle &= \cos\theta|0\rangle + \sin\theta|2\rangle\,, \\ |e, +; n_g\rangle &= \sin\theta|0\rangle - \cos\theta|2\rangle\,,\end{aligned} \tag{80}$$

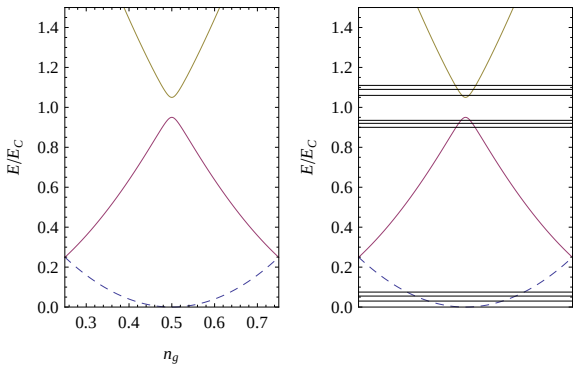

FIG. 3: Left panel: spectrum of the reduced CPB Hamiltonian, Eq. (75), around the operating point $n_g = 1/2$ for $E_J = 0.1E_C$. Dashed line: energy of the odd state, Eq. (77). Solid lines: energies of ground (bottom) and excited (top) even states, Eq. (78). Right panel: in the presence of a small inductive energy E_L, the CPB bands act as potentials in the quasimomentum space, see Ref. 14. Dense horizontal lines represent a few energy levels near the edges of the bands.

where

$$\cos\theta = \frac{1}{\sqrt{2}}\sqrt{1 - \frac{4E_C(2n_g-1)}{\omega_{10}(n_g)}}. \tag{81}$$

The non-vanishing matrix elements of $\sin\hat{\varphi}/2$ can be readily obtained using the charge basis form of this operator

$$\sin\frac{\hat{\varphi}}{2} = \frac{1}{2i}\sum_q \Big(|q+1\rangle\langle q| - |q\rangle\langle q+1|\Big). \tag{82}$$

For the states in Eqs. (76) and (80) we find

$$\left|\langle o, 0; n_g|\sin\frac{\hat{\varphi}}{2}|e, \pm; n_g\rangle\right|^2 = \frac{1}{4}\left[1 \pm \frac{E_J}{\omega_{10}(n_g)}\right]. \tag{83}$$

We stress that the transitions are not between the qubit (i.e., even) states, but between the even and odd states; the corresponding transition frequencies are $\omega_\pm(n_g) = E_C \pm \omega_{10}(n_g)/2$, see Eqs. (77) and (78). Therefore the tunneling of a quasiparticle into the CPB changes the parity of the state, an effect known as "quasiparticle poisoning".[6] Substituting the matrix element (83) into Eq. (32) and using the high-frequency expression (41) we find

$$\Gamma_{e,+\to o,0} = \left[1 + \frac{E_J}{\omega_{10}(n_g)}\right]\frac{2E_J}{\pi}\,x_{\rm qp}\sqrt{\frac{2\Delta}{\omega_+(n_g)}} \tag{84}$$

for the transition between even excited and odd states. In thermal equilibrium with $T \ll \omega_+(n_g)$, using Eq. (21) we obtain

$$\Gamma_{e,+\to o,0} = \left[1 + \frac{E_J}{\omega_{10}(n_g)}\right]\frac{4E_J}{\sqrt{\pi}}\sqrt{\frac{T}{\omega_+(n_g)}}e^{-\Delta/T}. \tag{85}$$

Within our approximations, this expression reproduces (after implementing the corrections described in Ref. 22 and up to a numerical prefactor) the decay rate calculated in Ref. 5 for the "open" qubit at the operating point $n_g = 1/2$. For the transition between even ground and odd states the matrix element in Eq. (83) vanishes at the operating point. This vanishing is a consequence of the low-energy approximation that lead to Eq. (6): as the results of Refs. 5,18 show, the contributions that we neglect cause a finite transition rate, which is suppressed by a small factor of order $E_C/2\Delta$ in comparison with the transition rate from even excited to odd state.

We note that while in all the above expressions the distance $|2n_g - 1|$ from the operating point can be large compared to the small parameter $E_J/E_C \ll 1$, the description based on Eq. (75) is valid if other charge states can be neglected, which limits the range of validity to $|2n_g - 1| < 1/2$ (with $|2n_g - 1| - 1/2 \gg E_J/E_C$). For example, at $2n_g - 1 \simeq 1/2$ the charge states $|0\rangle$ and $|3\rangle$ are nearly degenerate and we can expect an enhanced transition rate $\Gamma_{e,+\to o,3}$ in comparison to the rate $\Gamma_{e,+\to o,0}$ that we have considered above.

Finally, let us comment on the relationship between the transition rate in the CPB and in the inductively shunted Josephson junction with large charging energy [see the paragraph containing Eq. (59)]. As shown schematically in the right panel of Fig. 3 and discussed in detail in Ref. 14, the spectra of the two systems are distinct even in the limit of small inductive energy E_L: in the CPB ($E_L = 0$) the energy levels form bands as n_g varies, while for any non-zero E_L the gate voltage n_g can be "gauged away" and the spectrum consists of discrete levels that become denser as E_L decreases. Despite these differences, the ac responses of the two systems due to charge coupling agree in this limit.[14] Similarly, we now show agreement for the quasiparticle transition rates. We note that when taking the limit $E_L \to 0$, the condition $E_J \lesssim \omega_{LC}$ for the validity of Eq. (59) for the rate $\Gamma_{n\to 0}$ requires that we also take $E_J \to 0$.[23] Moreover, since the final state considered in deriving the rate $\Gamma_{n\to 0}$ is the lowest possible state, the corresponding final state in the CPB is either the even ground state at $n_g = 0$ or the odd ground state at $n_g = 1/2$. Indeed, the width of the ground state (in quasimomentum space – see Fig. 3 and Ref. 14) is $\propto (E_L/E_C)^{1/4}$, so that as $E_L \to 0$ the state is localized at the bottom of the band. Note that following the same procedure detailed above it is straightforward to show that the transition rate $\Gamma_{o,+\to e,0}$ at $n_g = 0$ coincides with $\Gamma_{e,+\to o,0}$ at $n_g = 1/2$; hence for our purposes the two possibilities are equivalent. At finite E_L, the total transition rate to the ground state is obtained by summing Eq. (59) over all initial levels n. Due to the Gaussian factor in the second line of Eq. (59), the number of levels that contribute to the total rate is approximately $\sqrt{n_0} \propto (E_C/E_L)^{1/4}$, which grows as the inductive energy diminishes. However, the energy of the contributing levels tends to the charging energy, as can be seen by rewriting identically the argument in the exponential of the Gaussian factor as $-(E_n - E_C)^2/2E_C\omega_{LC}$, where $E_n = n\omega_{LC}$; this agrees with frequency for the $e, + \to o, 0$ transition at $n_g = 1/2$ in the CPB being approximately E_C in the small E_J limit. Using Eq. (59), performing the sum over levels, and taking the limit $E_L \to 0$, we find

$$\lim_{E_L\to 0} \sum_n \Gamma_{n\to 0} = \frac{4E_J}{\pi}\, x_{\rm qp} \sqrt{\frac{2\Delta}{E_C}}\,, \qquad (86)$$

which coincides with the leading term of Eq. (84) in the limit $E_J \to 0$ at the operating point $n_g = 1/2$.

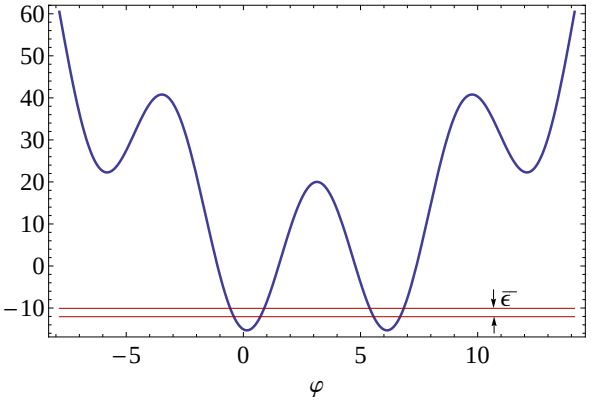

FIG. 4: Potential energy (in units of E_L) for a flux qubit biased at $\Phi_e = \Phi_0/2$ with $E_J/E_L = 10$. The horizontal lines represent the two lowest energy levels, with energy difference $\bar{\epsilon}$ given in Eq. (100).

B. Flux qubit

As a second example of a strongly anharmonic system, we consider here a flux qubit, i.e., in Eq. (2) we assume $E_J > E_L$ and take the external flux to be close to half the flux quantum, $\Phi_e \approx \Phi_0/2$. Then the potential has a double-well shape and the flux qubit ground states $|-\rangle$ and excited state $|+\rangle$ are the lowest tunnel-split eigenstates in this potential,[8] see Fig. 4. The non-linear nature of the $\sin\hat{\varphi}/2$ qubit-quasiparticle coupling in Eq. (6) has a striking effect on the transition rate $\Gamma_{+\to -}$, which vanishes at $\Phi_e = \Phi_0/2$ due to destructive interference: for flux biased at half the flux quantum the qubit states $|-\rangle$, $|+\rangle$ are respectively symmetric and antisymmetric around $\varphi = \pi$, while the potential in Eq. (2) and the function $\sin\varphi/2$ in Eq. (32) are symmetric. Note that the latter symmetry and its consequences are absent in the environmental approach in which a linear phase-quasiparticle coupling is assumed.

Analytic evaluation of the matrix element determining the transition rate [Eq. (32)] at finite $\Phi_e - \Phi_0/2$ is possible when $E_C \ll E_J$ and the tunnel splitting $\bar{\epsilon}$ is small compared to inductive and plasma energies, $\bar{\epsilon} \ll 2\pi^2 E_L \ll \omega_p$; an estimate for the splitting is given

below in Eq. (100). With the above assumptions we can use a tight-binding approach. Neglecting tunneling the wavefunctions $|m\rangle$ are, as a first approximation, ground state wavefunctions of the harmonic oscillator with frequency ω_p and oscillator length $\ell = \sqrt{8E_C/\omega_p}$ localized around the (flux-dependent) minima φ_m of the potential energy,

$$\langle\varphi|m\rangle = \left(\frac{1}{\pi\ell^2}\right)^{1/4} e^{-(\varphi-\varphi_m)^2/2\ell^2}. \tag{87}$$

The minima are found by solving Eq. (49) approximately, using the condition $E_L \ll E_J$ (which follows from the above assumptions) to get

$$\varphi_m \simeq 2\pi\left[m - \frac{E_L}{E_J}(m-f)\right], \qquad f = \frac{\Phi_e}{\Phi_0}. \tag{88}$$

The energies of the localized states are (up to a constant term)

$$E_m = 2\pi^2\bar{E}_L(m-f)^2, \tag{89}$$

where

$$\bar{E}_L = E_L\left(1-\frac{1}{\beta}\right), \qquad \beta = \frac{E_J}{E_L} \tag{90}$$

takes into account corrections small in $1/\beta \ll 1$. The above results are valid for $|mE_L/E_J| \ll 1$. Still neglecting tunneling, the matrix element of $\sin\hat{\varphi}/2$ between states localized in different wells vanishes, but the diagonal matrix element is finite due to the shift of the minima away from $2\pi m$, see Eq. (88). Using the states in Eq. (87) we obtain

$$\langle j|\sin\frac{\hat{\varphi}}{2}|m\rangle \simeq -(-1)^m\pi\frac{E_L}{E_J}(m-f)\delta_{m,j}. \tag{91}$$

To include the effect of tunneling we allow for the possibility of transitions between neighboring wells with amplitude $\bar{\epsilon}/2$. As we are interested in the two lowest eigenstates for f near $1/2$, we consider only the $m = 0, 1$ wells and the effective Hamiltonian has the form

$$\hat{H} = \begin{pmatrix} 2\pi^2\bar{E}_L f^2 & -\bar{\epsilon}/2 \\ -\bar{\epsilon}/2 & 2\pi^2\bar{E}_L(1-f)^2 \end{pmatrix}. \tag{92}$$

The eigenenergies are [cf. Eqs. (78)-(81)]

$$E_\pm(f) = \frac{\pi^2}{2}\bar{E}_L\left[1+(2f-1)^2\right] \pm \frac{1}{2}\omega_{10}(f) \tag{93}$$

with the flux-dependent qubit frequency

$$\omega_{10}(f) = \sqrt{\bar{\epsilon}^2 + \left[(2\pi)^2\bar{E}_L(f-1/2)\right]^2}, \tag{94}$$

while the eigenstates are

$$\begin{aligned} |-\rangle &= \cos\theta|0\rangle + \sin\theta|1\rangle, \\ |+\rangle &= \sin\theta|0\rangle - \cos\theta|1\rangle, \end{aligned} \tag{95}$$

with

$$\cos\theta = \frac{1}{\sqrt{2}}\sqrt{1 - \frac{(2\pi)^2\bar{E}_L(f-1/2)}{\omega_{10}(f)}}. \tag{96}$$

The tunnel splitting $\bar{\epsilon}$ entering in the above formulas can be estimated by noting that due to the assumption $\beta \gg 1$ the wells are nearly symmetric. Neglecting the asymmetry [i.e., considering the potential in Eq. (2) at $f = 1/2$], the width and height of the tunnel barrier are approximately $2\pi(1-1/\beta)$ and $2\bar{E}_J$, respectively, with

$$\bar{E}_J = E_J\left[1 - \frac{\pi^2}{4}\frac{1}{\beta}\left(1-\frac{1}{\beta}\right)\right]. \tag{97}$$

To account for the height and width at $E_L \neq 0$, we treat the two wells as cosine potentials with renormalized coefficients. That is, we consider each well to be described by the Hamiltonian given in Eq. (B3) with the substitutions $E_J \to \bar{E}_J$ and $E_C \to \bar{E}_C$, where

$$\bar{E}_C = E_C\frac{1}{(1-1/\beta)^2}. \tag{98}$$

Then we can use the known asymptotic formula[2,14,24] for the splitting ϵ_0 in the periodic cosine potential (i.e., for $E_L = 0$; see Appendix B for a derivation of this formula)

$$\epsilon_0 = 4\sqrt{\frac{2}{\pi}}\omega_p\left(\frac{8E_J}{E_C}\right)^{1/4} e^{-\sqrt{8E_J/E_C}} \tag{99}$$

to find

$$\bar{\epsilon} = 2\sqrt{\frac{2}{\pi}}\sqrt{8\bar{E}_J\bar{E}_C}\left(\frac{8\bar{E}_J}{\bar{E}_C}\right)^{1/4} e^{-\sqrt{8\bar{E}_J/\bar{E}_C}}. \tag{100}$$

Here the numerical prefactor is smaller by factor of 2 in comparison with Eq. (99) to account for tunneling being between two wells rather than in a periodic potential.[24]

Turning now to the matrix element $\langle j|\sin\hat{\varphi}/2|m\rangle$, the diagonal elements $j = m = 0, 1$ are still approximately given by Eq. (91). Tunneling introduces finite but exponentially small off-diagonal elements which, similarly to the splitting, can be calculated using the semiclassical approximation. Using the wavefunctions derived in Appendix B we arrive at [cf. Eq. (C6)]

$$\langle 1|\sin\frac{\hat{\varphi}}{2}|0\rangle \simeq D\left(\frac{\bar{E}_J}{\bar{E}_C}\right)^{1/3}\frac{\bar{\epsilon}}{2\sqrt{2}\bar{E}_J} \tag{101}$$

with $D \approx 1.45$, see Eq. (C7). We can now calculate the matrix element of $\sin\hat{\varphi}/2$ between qubit states $|\pm\rangle$ in Eq. (95) using Eqs. (91) and (101) to obtain

$$\begin{aligned} \langle -|\sin\frac{\hat{\varphi}}{2}|+\rangle &= \pi(f-1/2)\frac{\bar{\epsilon}}{\omega_{10}(f)} \\ &\times\left[\frac{E_L}{E_J} + \sqrt{2}\pi D\frac{\bar{E}_L}{\bar{E}_J}\left(\frac{\bar{E}_J}{\bar{E}_C}\right)^{1/3}\right]. \end{aligned} \tag{102}$$

Here the first term in square brackets is the combination of the two intrawell contributions [Eq. (91)] while the second one originates from the under-barrier tunneling [Eq. (101)]. Comparing Eq. (102) to numerical calculations, we find that near half the flux quantum, $|f-1/2| \lesssim \bar{\epsilon}/2\pi^2 E_L$, the two approaches give the same dependence on flux and agree on the order of magnitude of the matrix element, with Eq. (102) providing a smaller estimate than the numerics by a factor of about 2/3. For $|f-1/2| \gtrsim \bar{\epsilon}/(2\pi)^2 E_L$ the flux dependence in Eq. (102) via the factor $(f-1/2)/\omega_{10}(f)$ can be neglected and the right hand side reduces to a flux-independent constant. However, this behavior is an artifact of our approximations: for these larger deviations of flux from half the flux quantum the matrix element acquires additional flux dependence, beyond that given in Eq. (102), once the asymmetry of the potential is taken into account. Moreover, for very small flux, $|f| \lesssim (\bar{\epsilon}/4\sqrt{2}\pi^2 E_L)^2$, mixing of the sate localized in well $m=1$ with that localized in well $m=-1$ cannot be neglected and the matrix element has a narrow peak around zero flux. Substituting Eq. (102) into Eq. (32), keeping the leading contribution, and using the relation (40), we find for the transition rate in the high-frequency regime[25]

$$\Gamma_{+\to-} = \frac{\omega_{10}}{\pi}\frac{1}{g_K}\mathrm{Re}\, Y_{\rm qp}^{hf}(\omega_{10})\left(\frac{\bar{\epsilon}}{4\pi\bar{E}_J}\right)^2\left(1-\frac{\bar{\epsilon}^2}{\omega_{10}^2}\right)\left(\sqrt{2}\pi D\right)^2\left(\frac{\bar{E}_J}{\bar{E}_C}\right)^{2/3} \tag{103}$$

with $\mathrm{Re}\, Y_{\rm qp}^{hf}$ of Eq. (18).

The rate in Eq. (103) depends on reduced flux f via the qubit frequency, see Eq. (94). In particular, for external flux equaling half the flux quantum we have $\omega_{10}(1/2) = \bar{\epsilon}$ and the transition rate vanishes, as discussed above. In the previous section we mentioned in the text after Eq. (85) that for the Cooper pair box the vanishing of the rate at the operating point is valid up to small corrections, being a consequence of the low-energy approximation for the tunneling Hamiltonian in Eq. (6). The same is true for the flux qubit; in the present case, the parameter suppressing these corrections is exponentially small, being given by $\bar{\epsilon}/2\Delta$. Note that if keeping in Eq. (5) the contributions beyond the low energy approximation, the operators accounting for the qubit-quasiparticle interaction cannot be reduced to $\sin\hat{\varphi}/2$; therefore, for these additional contributions the symmetry argument given at the beginning of this section for the vanishing of the transition rate at $f=1/2$ does not hold.

V. MULTIPLE-JUNCTION QUBITS: GENERAL THEORY AND APPLICATIONS

In this section we generalize the theory of Sec. II to the case of systems containing multiple junctions. This generalization will enables us to consider the flux dependence of the transition rates in the two-junction split transmon and in the many-junction fluxonium. These two qubits are particular examples of the general case in which $M+1$ junctions separate $M+1$ superconducting islands forming a loop. We use the convention that junction $j=0,\ldots,M$ is between islands j and $j+1$ and identify island $j=M+1$ with island $j=0$ – see Fig. 5. When the loop inductive energy is much larger than the Josephson energies of the junctions (i.e., the loop inductance is small), the phases are subject to the flux quantization constraint

$$\sum_{j=0}^{M}\varphi_j = 2\pi\Phi_e/\Phi_0\,. \tag{104}$$

This constraint must be taken into account to derive the Hamiltonian $\hat{H}_{\{\phi\}}$ of the M independent phase degrees of freedom ϕ, ϕ_k $(k=1,\ldots,M-1)$ starting from the Lagrangian[26] $\mathcal{L}_{\{\varphi\}}$ for the $M+1$ constrained phases φ_j

$$\mathcal{L}_{\{\varphi\}} = \sum_{j=0}^{M}\left[\frac{1}{2}C_j\left(\frac{\Phi_0}{2\pi}\dot{\varphi}_j\right)^2 + E_{Jj}\cos\varphi_j\right], \tag{105}$$

where the dot denotes derivative with respect to time, C_j is the capacitance of junction j, and E_{Jj} its Josephson energy. In Appendix F we derive the Hamiltonian assuming M of the $M+1$ junctions to be identical, which is relevant for both the split transmon ($M=1$) and the fluxonium ($M\gg1$). Explicit expressions for the Hamiltonian in these two cases are presented below.

The total Hamiltonian $\hat{H}$ of the system consist of three terms, as in Eq. (1):

$$\hat{H} = \hat{H}_{\{\phi\}} + \hat{H}_{\rm qp} + \hat{H}_T\,. \tag{106}$$

In addition to $\hat{H}_{\{\phi\}}$ discussed above, the second contribution is the quasiparticle Hamiltonian

$$\hat{H}_{\rm qp} = \sum_{j=0}^{M}\hat{H}_{\rm qp}^j\,, \quad \hat{H}_{\rm qp}^j = \sum_{n,\sigma}\epsilon_n^j\hat{\alpha}_{n\sigma}^{j\dagger}\hat{\alpha}_{n\sigma}^j\,. \tag{107}$$

Here the index j denotes the superconducting island; other symbols have the same meaning as in Eq. (3) and we assume equal gaps in all islands, $\Delta^j\equiv\Delta$. The final contribution to $\hat{H}$ is the tunnel Hamiltonian, given by the following sum [cf. Eq. (6)]

$$\hat{H}_T = \sum_{j=0}^{M}\tilde{t}_j\sum_{n,m,\sigma} i\sin\frac{\hat{\varphi}_j}{2}\hat{\alpha}_{n\sigma}^{j\dagger}\hat{\alpha}_{m\sigma}^{j+1} + \mathrm{H.c.} \tag{108}$$

The transition rate between qubit states can again be calculated using Fermi's golden rule as in Eq. (31). We assume that the quasiparticle distribution functions are the same in all islands and that tunneling across each junction is not correlated with tunneling in nearby junctions – this is a good assumption if the mean level spacing in the finite size superconductors is small compared

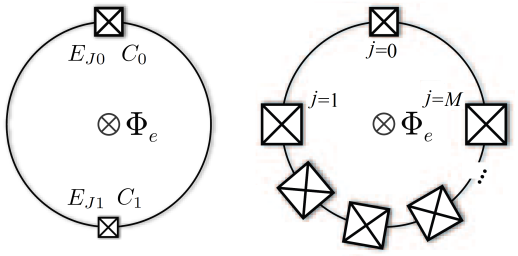

FIG. 5: Left: schematic representation of the split transmon with two (possibly different) junctions. Right: in the fluxonium a weaker junction ($j = 0$) is connected to a large junction array ($j = 1, \ldots, M$).

to the gap. Then the total rate for the transition between eigenstates of Hamiltonian $\hat{H}_{\{\phi\}}$ is

$$\Gamma_{i\to f} = \sum_{j=0}^{M} \left| \langle f_{\{\phi\}} | \sin \frac{\hat{\varphi}_j}{2} | i_{\{\phi\}} \rangle \right|^2 E_{Jj} \tilde{S}_{\rm qp}\left(\omega_{if}\right), \quad (109)$$

where for convenience we have extracted the Josephson energy prefactor from the spectral density, $\tilde{S}_{\rm qp} = S_{\rm qp}/E_J$, with $S_{\rm qp}$ defined in Eq. (33). Similarly, the correction δE_i to the energy of state $i_{\{\phi\}}$ is given by sums over junctions which generalize Eqs. (45) and (46),

$$\delta E_i = \delta E_{i,E_J} + \delta E_{i,\rm qp}\,, \quad (110)$$

$$\delta E_{i,E_J} = \sum_{j=0}^{M} E_{Jj} \langle i_{\{\phi\}} | \cos\hat{\varphi}_j | i_{\{\phi\}} \rangle (x_{\rm qp} + 2x_{\rm qp}^{\rm A})\,, \quad (111)$$

$$\delta E_{i,\rm qp} = \sum_{j=0}^{M} E_{Jj} \sum_{k\neq i} \left| \langle k_{\{\phi\}} | \sin \frac{\hat{\varphi}_j}{2} | i_{\{\phi\}} \rangle \right|^2 \tilde{F}_{\rm qp}(\omega_{ik}), \quad (112)$$

where $\tilde{F}_{\rm qp} = F_{\rm qp}/E_J$. In the next subsections we use Eq. (109) to calculate the transition rates for the split transmon and the fluxonium, and Eq. (110) to find the frequency shift in the split transmon. The flux-dependent transition rate between the two lowest even and odd states of a split Cooper pair box has been recently considered in Ref. 27 for gate voltage tuned at the operating point.

A. Split transmon

A split transmon consists of two junctions, $j = 0, 1$, in a superconducting loop, see Fig. 5. Therefore, there is only $M = 1$ degree of freedom, which we denote with ϕ, governed by the Hamiltonian

$$\hat{H}_\phi = 4E_C\hat{N}^2 - E_{J0}\cos(\hat{\phi} - 2\pi f) - E_{J1}\cos\hat{\phi}\,, \quad (113)$$

see Appendix F. Here $\hat{N} = -id/d\phi$, $f = \Phi_e/\Phi_0$, and the charging energy E_C is related to the junctions' capacitances by

$$E_C = \frac{e^2}{2(C_0 + C_1)}\,. \quad (114)$$

Note that the Hamiltonian is periodic in f with period 1, so we can assume $|f| \leq 1/2$ without loss of generality (i.e., we can measure the normalized flux from the nearest integer). After shifting $\phi \to \phi + \pi f$, the sum of the two Josephson terms can be rewritten as

$$E_{J0}\cos(\hat{\phi} - 2\pi f) + E_{J1}\cos\hat{\phi} \to E_J(f)\cos(\hat{\phi} - \vartheta)\,, \quad (115)$$

where the effective Josephson energy E_J is modulated by the external flux

$$E_J(f) = (E_{J0} + E_{J1})\cos(\pi f)\sqrt{1 + d^2\tan^2(\pi f)} \quad (116)$$

with

$$d = \frac{E_{J0} - E_{J1}}{E_{J0} + E_{J1}} \quad (117)$$

and

$$\tan\vartheta = d\tan(\pi f). \quad (118)$$

After a further shift $\phi \to \phi + \vartheta$ we arrive at

$$\hat{H}_\phi = 4E_C\hat{N}^2 - E_J(f)\cos\hat{\phi}\,, \quad (119)$$

which has the same form of the Hamiltonian for the single junction transmon [i.e., Eq. (2) with $E_L = 0$] but with a flux-dependent Josephson energy, Eq. (116). Therefore the spectrum follows directly from that of the single junction transmon (see Fig. 2) and consists of nearly degenerate and well separated states. The energy difference between well separated states is approximately given by the flux-dependent frequency [cf. Eq. (56)]

$$\omega_p(f) = \sqrt{8E_C E_J(f)}. \quad (120)$$

Note that for the system to be in the transmon regime

$$E_J(f) \gg E_C \quad (121)$$

at some flux, a necessary condition is

$$E_{J0} + E_{J1} \gg E_C\,. \quad (122)$$

Then we can distinguish two cases. First, in the nearly symmetric case of junctions with comparable Josephson energies, $|E_{J0} - E_{J1}| \lesssim E_C$, the condition (121) is satisfied not too close to half the flux quantum,

$$|f| - 1/2 \gg E_C/\pi(E_{J0} + E_{J1}). \quad (123)$$

On the other hand, if the Josephson energies are sufficiently different, $|E_{J0} - E_{J1}| \gg E_C$, then Eq. (121) is satisfied at any flux.

The transition rate $\Gamma_{1\to0}$ between the qubit states $|0\rangle$, $|1\rangle$ can be calculated using Eq. (109) if we know the relation between φ_j and ϕ; the same relation is also needed to calculate the transition rate $\Gamma_{o\to e}$ between nearly degenerate states – see Appendix C 2 for details. According to Appendix F, for the variable ϕ in Eq. (113) we have $\varphi_1 = \phi$ and $\varphi_0 = 2\pi f - \phi$. Accounting for the two changes of variables performed to arrive at Eq. (119) we obtain

$$\begin{aligned}\hat{\varphi}_0 &= \pi f - \vartheta - \hat{\phi}\,,\\ \hat{\varphi}_1 &= \pi f + \vartheta + \hat{\phi}\,.\end{aligned} \tag{124}$$

In the transmon regime (121), we proceed as in the derivation of Eq. (53) to find

$$\left|\langle 0|\sin\frac{\hat{\varphi}_j}{2}|1\rangle\right|^2 = \frac{E_C}{\omega_p(f)}\frac{1+\cos(\pi f\pm\vartheta)}{2}\,, \tag{125}$$

where the upper (lower) sign is to be used for $j=1$ ($j=0$). Substituting this result into Eq. (109) and using Eq. (41) with $\omega=\omega_p(f)$, we find in the high frequency regime [cf. Eq. (55)]

$$\Gamma_{1\to0} = \frac{x_{\rm qp}}{2\pi}\sqrt{\frac{2\Delta}{\omega_p(f)}}\frac{\omega_p^2(f)+\omega_p^2(0)}{\omega_p(f)}\,. \tag{126}$$

For the transition quality factor we consider, as in Sec. III A, the coexistence of equilibrium and non-equilibrium quasiparticles [see Eq. (61)] to find

$$\begin{aligned}\frac{1}{Q_{10}} = \frac{1}{2\pi}\left(1+\frac{\omega_p^2(0)}{\omega_p^2(f)}\right)\Bigg[x_{ne}\sqrt{\frac{2\Delta}{\omega_p(f)}}\\ +4e^{-\Delta/T}\cosh\left(\frac{\omega_p(f)}{2T}\right)K_0\left(\frac{\omega_p(f)}{2T}\right)\Bigg].\end{aligned} \tag{127}$$

In Fig. 6 we show with solid lines the quality factor as function of temperature for 4 different values of flux f in a symmetric transmon (d=0). As we discussed in Sec. III A, an extrinsic relaxation mechanism could be limiting the low temperature quality factor. Characterizing this mechanism by a constant quality factor $Q_{\rm ext}$ and assuming that only equilibrium quasiparticles are present, the transition quality factor has the form

$$\begin{aligned}\frac{1}{Q_{10,\rm tot}} = \frac{1}{Q_{\rm ext}} + \frac{2}{\pi}\left(1+\frac{\omega_p^2(0)}{\omega_p^2(f)}\right)\\ \times e^{-\Delta/T}\cosh\left(\frac{\omega_p(f)}{2T}\right)K_0\left(\frac{\omega_p(f)}{2T}\right).\end{aligned} \tag{128}$$

The dashed lines in Fig. 6 show $Q_{10,\rm tot}$ as a function of temperature for the same values of flux; the quality factor $Q_{\rm ext}$ is chosen so that the zero-flux curve coincides with the zero flux-curve described by Eq. (127). The change of quality factor with flux is markedly different in the two limiting cases (namely, presence of non-equilibrium quasiparticles and no extrinsic relaxation mechanism vs.

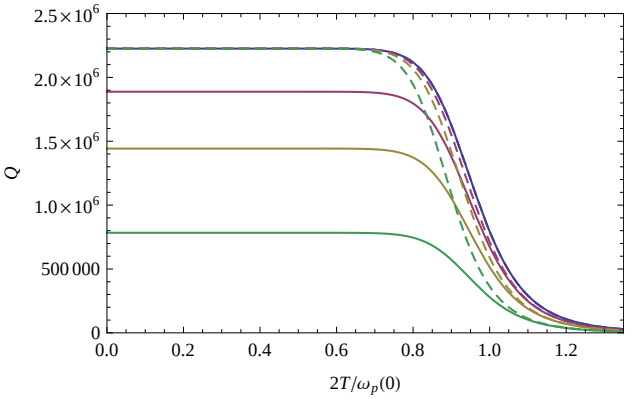

FIG. 6: Quality factor as function of $2T/\omega_p(0)$ in a symmetric split transmon. Solid lines are obtained from Eq. (127) using a small nonequilibrium quasiparticle density $x_{ne}=3.8\times10^{-7}$ and a gap value such that $\Delta/\omega_p(0)=6.9$ (these parameters are taken from experiments on single junction transmon[20]). Flux increases from top to bottom; we show curves for $f=0$, 0.2, 0.3, and 0.4, respectively. We plot Eq. (128) with dashed lines for the same values of flux. The extrinsic quality factor is chosen so that solid and dashed lines match at $f=0$.

extrinsic relaxation with no non-equilibrium quasiparticles) described by Eqs. (127) and (128). Therefore the measurement of the temperature and flux dependencies of the quality factor should give indications on the presence of non-equilibrium quasiparticles. For example, the low-temperature measurements reported in Ref. 28 are compatible with a flux-independent quality factor; to explain the data with Eq. (127) rather than Eq. (128) one would need to assume a quasiparticle density that decreases with increasing flux. Since magnetic fields are known to break pairs and thus increase the quasiparticle density, for the transmons considered in Ref. 28 it is unlikely that non-equilibrium quasiparticles are the source of the low-temperature qubit decay.

The frequency shift for the split transmon is obtained, as in Sec. III B, by calculating the difference between correction to energies of nearby levels, Eq. (67). The matrix elements appearing in Eqs. (111)-(112) are given by Eqs. (53) and (69) with $\omega_{10}=\omega_p(f)$, $\varphi_0=\theta+\pi f$ for $j=1$, and $\varphi_0=\theta-\pi f$ for $j=0$ [cf. Eq. (124)-(125)]. Using those expressions we find

$$\delta E_{i+1,E_J} - \delta E_{i,E_J} = -\frac{1}{2}\omega_p(f)\left(x_{\rm qp}+2x_{\rm qp}^{\rm A}\right) \tag{129}$$

and

$$\begin{aligned}\delta E_{i+1,\rm qp} - \delta E_{i,\rm qp} = \frac{1}{16}\frac{\omega_p^2(0)+\omega_p^2(f)}{\omega_p(f)}\\ \left[\tilde{F}_{\rm qp}(\omega_p(f))+\tilde{F}_{\rm qp}(-\omega_p(f))\right].\end{aligned} \tag{130}$$

Then using the relation (48) and Eq. (29), we arrive at

the high frequency result

$$\frac{\delta\omega(f)}{\omega_p(f)} = \frac{1}{2}\left\{ x_{\rm qp}^{\rm A}\left(\frac{\omega_p^2(0)}{\omega_p^2(f)}-1\right) - x_{\rm qp}\left[\frac{1}{2\pi}\left(\frac{\omega_p^2(0)}{\omega_p^2(f)}+1\right)\sqrt{\frac{2\Delta}{\omega_p(f)}}+1\right]\right\}. \tag{131}$$

At zero flux this expression agrees with Eq. (73) applied to a single junction transmon ($\omega_{10}=\omega_p$, $\varphi_0=0$). However, similarly to the flux qubit, at finite flux the split transmon frequency shift is sensitive to the occupation of the Andreev bound states, see the first term in curly brackets.

B. Fluxonium

In the fluxonium, an array of many identical junctions ($M\gg 1$) of Josephson energy $E_{J1}\gg E_{C1}$ is connected to a weaker junction with $E_{J0}<E_{J1}$. Then the Hamiltonian $\hat H_{\{\phi\}}$ for the M independent degrees of freedom can be approximately separated into independent terms for the qubit phase ϕ and the $M-1$ phases ϕ_k,

$$\begin{aligned}\hat H_{\{\phi\}} &= \hat H_\phi + \sum_{k=1}^{M-1}\hat H_k\,, \\ \hat H_\phi &= 4E_C\hat N^2 - E_{J0}\cos\hat\phi + \frac{1}{2}E_L(\hat\phi-2\pi f)^2, \\ \hat H_k &= 4E_{C1}\hat N_k^2 + \frac{1}{2}E_{J1}\hat\phi_k^2\,,\end{aligned} \tag{132}$$

where

$$E_L = \frac{E_{J1}}{M}, \qquad \frac{1}{E_C}=\frac{1}{E_{C0}}+\frac{1}{ME_{C1}}, \tag{133}$$

see Appendix F. There, we also give [Eq. (F5)] the relation between the $M+1$ (constrained) φ_j variables and the M independent ϕ_k variables. Accounting for the changes of variables that bring the Hamiltonian in the form given above, we have schematically

$$\begin{aligned}&\varphi_0=\phi\,,\\ &\varphi_j = L_j(\{\phi_k\}) + (2\pi f-\phi)/M\,, \qquad j=1,\dots,M\,.\end{aligned} \tag{134}$$

Here $L_j(\{\phi_k\})$ denote linear combinations of the variables ϕ_k, $k=1,\dots,M-1$, whose specific form can be found in Appendix F but is not needed here, while we show explicitly the dependence of the constrained variables φ_j on the qubit phase ϕ. As in the previous section, we take $|f|<1/2$ without loss of generality.

As an example of the calculation of the transition rate for such a system, we assume that the plasma frequency $\omega_{p1}=\sqrt{8E_{C1}E_{J1}}$ of the array junctions is larger than the other relevant energy scales (namely, quasiparticle energy δE and qubit frequency ω_{10}). Then we can take the many-body state of the system $|\Psi_{\{\phi\}}\rangle$ in the product form

$$|\Psi_{\{\phi\}}\rangle = |\psi_\phi\rangle\prod_{k=1}^{M-1}|0_k\rangle, \tag{135}$$

where $|\psi_\phi\rangle$ is a low-energy eigenstate of $\hat H_\phi$ and $|0_k\rangle$ is the ground state wave function of the kth oscillator. The approximations used to derive $\hat H_{\{\phi\}}$ in Eq. (132) imply that in the formula (109) for the transition rate we can linearize the sine for $j=1,\dots,M$. Therefore, for the transition rate between two states of the form (135) we obtain

$$\Gamma_{i\to f} = \tilde S_{\rm qp}(\omega_{if})\left[E_{J0}\left|\langle f_\phi|\sin\frac{\hat\phi}{2}|i_\phi\rangle\right|^2 + E_L\left|\langle f_\phi|\frac{\hat\phi}{2}|i_\phi\rangle\right|^2\right]. \tag{136}$$

In the weak tunneling limit $\bar\epsilon \ll 2\pi^2E_L \ll \omega_p = \sqrt{8E_CE_{J0}}$ (with $\bar\epsilon$ the tunnel splitting of the qubit states at $f=1/2$), we can use directly the results of Sec. IV B: the flux-dependent qubit frequency $\omega_{10}(f)$ is given by Eq. (94) and the first excited state $|i_\phi\rangle=|+\rangle$ and ground state $|f_\phi\rangle=|-\rangle$ are the linear combination of states localized in wells $m=0$, 1 in Eq. (95). For the first term in square brackets in Eq. (136), the matrix element is given by Eq. (102). To evaluate the second term in the same regime, we note that for states $|m\rangle$, $|j\rangle$ – that is, states localized in wells m and j as in Eq. (87) – we have

$$\langle j|\frac{\hat\phi}{2}|m\rangle = \pi\left[m\left(1-\frac{E_L}{E_{J0}}\right)+\frac{E_L}{E_{J0}}f\right]\delta_{j,m}\,. \tag{137}$$

Therefore for the states in Eq. (95) we find

$$\left|\langle-|\frac{\hat\phi}{2}|+\rangle\right|^2 = \left(\frac{\pi}{2}\right)^2\left(1-\frac{E_L}{E_{J0}}\right)^2\frac{\bar\epsilon^2}{\omega_{10}^2(f)}\,. \tag{138}$$

In contrast to the matrix element of $\sin\hat\varphi/2$ considered in Sec. IV B, the contribution due to tunneling can be neglected in this case. Substituting this result and the leading term from Eq. (102) into the square brackets of Eq. (136) we get[29]

$$\frac{\pi^2}{4}\frac{\bar\epsilon^2}{\omega_{10}^2(f)}E_L\left[(2\pi)^2\frac{E_L}{E_{J0}}\left(f-\frac{1}{2}\right)^2\left(\sqrt{2}D\right)^2\left(\frac{E_{J0}}{E_C}\right)^{2/3} + \left(1-\frac{E_L}{E_{J0}}\right)^2\right]. \tag{139}$$

In this expression, the first term in square brackets originates from the weak junction and the second one from the array. Note that when considering flux near half the flux quantum we can neglect the first term in comparison

to the second and the losses due to the array dominate over those due to the weak junction. Keeping only the leading contribution in Eq. (139) and using Eq. (41) in Eq. (136), we arrive at the expression for the rate in the high-frequency regime

$$\Gamma_{+\to-} = x_{\rm qp}\sqrt{\frac{2\Delta}{\omega_{10}(f)}}\,2\pi E_L\,\frac{\omega_{10}^2(1/2)}{\omega_{10}^2(f)} \tag{140}$$

with $\omega_{10}(f)$ defined in Eq. (94). Note that since the frequency increases as the reduced flux f moves away from 1/2, the transition rate is the largest at half the flux quantum.

VI. SUMMARY

In this work we have presented in detail a general approach to study the effects of quasiparticles on relaxation and frequency of superconducting qubits. The theory is applicable to any qubit – the case of single-junction systems is considered in Sec. II and the generalization to multi-junction ones is given in Sec. V. Our analysis is valid for both thermal equilibrium quaisparticles and arbitrary non-equilibrium distributions, so long as the quasiparticle energy is small compared to the qubit frequency – this condition, not necessary in thermal equilibrium, ensures that quasiparticles primarily cause relaxation and not excitation of the qubit.

For single-junction qubits, we have studied in Sec. III the weakly anharmonic limit. For small phase fluctuations, both quality factor (Sec. III A) and frequency shift (Sec. III B) are determined by transitions between neighboring qubit levels and can be related to real and imaginary part of the "classical" junction admittance, respectively. The small fluctuation case applies to phase and transmon qubits and our results in Eqs. (62) and (73) have been successfully tested in recent experiments[20,21] with these qubits. For strong anharmonicity, we have presented in Sec. IV results for the quasiparticle transition rate in the Cooper pair box and the flux qubit.

We have considered two examples of multi-junction qubits, the two-junction split transmon in Sec. V A and the many-junction fluxonium in Sec. V B. In particular, we argue that measuring the temperature and flux dependencies of the quality factor of a split transmon could help resolve the question of wether non-equilibrium quasiparticles are present at low temperatures, see Eqs. (127)-(128) and Fig. 6.

Acknowledgments

We thank L. Frunzio, A. Kamal, and J. Koch for stimulating discussions and help with numerical calculations. This research was funded by DOE (Contract DE-FG02-08ER46482), by Yale University, and by the Office of the Director of National Intelligence (ODNI), Intelligence Advanced Research Projects Activity (IARPA), through the Army Research Office (Contract No. W911NF-09-1-0369). All statements of fact, opinion or conclusions contained herein are those of the authors and should not be construed as representing the official views or policies of IARPA, the ODNI, or the U.S. Government.

Appendix A: Correction to energy levels

To calculate the correction to the energy levels as presented in Sec. II C, we must account for both quasiparticle and pair tunneling. Note that due to energy conservation the latter does not affect the transition rate $\Gamma_{i\to f}$ between states $|i\rangle$ and $|f\rangle$ so long as $\omega_{if} < 2\Delta$; for this reason the pair tunneling Hamiltonian $\hat{H}_T^p$ was neglected in Eq. (1). More generally, the total Hamiltonian of the single junction system is

$$\hat{H}_{\rm tot} = \hat{H}_0 + \hat{H}_T + \hat{H}_T^p + \hat{H}_{E_J} \tag{A1}$$

with

$$\hat{H}_0 = \hat{H}_\varphi + \hat{H}_{\rm qp}\,. \tag{A2}$$

The Hamiltonians $\hat{H}_\varphi$, $\hat{H}_{\rm qp}$, and $\hat{H}_T$ are defined in Eqs. (2), (3), and (5), respectively, and the pair tunneling term is

$$\begin{aligned}\hat{H}_T^p = \tilde{t}\sum_{n,m}\Big[&\left(e^{i\frac{\hat{\varphi}}{2}}u_n^L v_m^R + e^{-i\frac{\hat{\varphi}}{2}}u_m^R v_n^L\right)\hat{\alpha}_{n\uparrow}^{L\dagger}\hat{\alpha}_{m\downarrow}^{R\dagger}\\ &+\left(e^{-i\frac{\hat{\varphi}}{2}}v_m^R u_n^L + e^{i\frac{\hat{\varphi}}{2}}v_n^L u_m^R\right)\hat{\alpha}_{m\downarrow}^{R}\hat{\alpha}_{n\uparrow}^{L}\Big] + (L\leftrightarrow R).\end{aligned} \tag{A3}$$

The last term in Eq. (A1),

$$\hat{H}_{E_J} = E_J\cos\hat{\varphi}\,, \tag{A4}$$

is necessary to avoid "double counting": the Josephson energy originates from pair tunneling, so its inclusion in the effective Hamiltonian $\hat{H}_\varphi$, Eq. (2), must be compensated for by subtracting the same term here. We will show below that this treatment is justified for small quasiparticle density.

In both the quasiparticle tunneling Hamiltonian $\hat{H}_T$, Eq. (5), and the pair tunneling one in Eq. (A3), using the definitions given after Eq. (3) the (real) Bogoliubov amplitudes are

$$\left(u_n^j\right)^2 = 1 - \left(v_n^j\right)^2 = \frac{1}{2}\left(1 + \frac{\xi_n^j}{\epsilon_n^j}\right), \qquad j = L, R\,. \tag{A5}$$

As in the main text, we assume equal gaps and distribution functions in the leads, $\Delta^L = \Delta^R \equiv \Delta$ and $f^L = f^R \equiv f$. Moreover, we neglect the contributions of the charge mode $f_Q(\epsilon) = (f(\xi) - f(-\xi))/2$, since they are suppressed by the small factor $\delta E/\Delta \ll 1$ compared to the leading contributions due to the energy mode f_E,

Eq. (14); for simplicity, in this Appendix we drop the subscript E.

We want to evaluate the correction δE_i to the energy of level i of the qubit at second order in the tunneling amplitude $\tilde{t}$ for small quasiparticle density. Thus, $\hat{H}_0$ in Eq. (A2) is the unperturbed Hamiltonian, and we distinguish three contributions to δE_i,

$$\delta E_i = \delta E_i^{(1)} + \delta E_i^{(2)} + \delta E_i^{(3)}, \tag{A6}$$

caused respectively by $\hat{H}_T$, $\hat{H}_T^p$, and $\hat{H}_{E_J}$. Noting that the latter is already of second order in $\tilde{t}$, we treat it within first order perturbation theory to write

$$\delta E_i^{(3)} = E_J \langle i| \cos\hat{\varphi} |i\rangle \,. \tag{A7}$$

The quasiparticle tunneling correction $\delta E_i^{(1)}$ is obtained by second order perturbation theory,

$$\delta E_i^{(1)} = -\sum_{k,\{\lambda\}_{\rm qp}} \langle\!\langle \frac{|\langle k,\{\lambda\}_{\rm qp}|\hat{H}_T|i,\{\eta\}_{\rm qp}\rangle|^2}{E_{\lambda,\rm qp} - E_{\eta,\rm qp} - \omega_{ik}} \rangle\!\rangle_{\rm qp} \,, \tag{A8}$$

where

$$\omega_{ik} = E_k - E_i \tag{A9}$$

and the notation is the same as in Sec. II: $\{\eta\}_{\rm qp}$ and $\{\lambda\}_{\rm qp}$ denote quasiparticle states, $E_{\lambda,\rm qp}$ and $E_{\eta,\rm qp}$ their energies, and $\langle\!\langle \ldots \rangle\!\rangle_{\rm qp}$ averaging over $\{\eta\}_{\rm qp}$. Performing the averaging, after lengthy but straightforward algebra we arrive at

$$\begin{aligned}\delta E_i^{(1)} = \frac{4E_J}{\pi^2\Delta} P \sum_k \int_{\Delta_{\rm qp}}^\infty d\epsilon_L \int_{\Delta_{\rm qp}}^\infty d\epsilon_R \\ \left[\left| \langle k| \sin\frac{\hat{\varphi}}{2} |i\rangle \right|^2 A_+(\epsilon_L,\epsilon_R) + \left| \langle k| \cos\frac{\hat{\varphi}}{2} |i\rangle \right|^2 A_-(\epsilon_L,\epsilon_R) \right] \\ \times \left[\frac{f(\epsilon_L)(1-f(\epsilon_R))}{\epsilon_L - \epsilon_R - \omega_{ik}} - \frac{(1-f(\epsilon_L))f(\epsilon_R)}{\epsilon_L - \epsilon_R + \omega_{ik}} \right],\end{aligned} \tag{A10}$$

where we introduced the functions

$$\begin{aligned}A_\pm(\epsilon_L,\epsilon_R) = \frac{\epsilon_L}{\sqrt{\epsilon_L^2 - \Delta_{\rm qp}^2}} \frac{\epsilon_R}{\sqrt{\epsilon_R^2 - \Delta_{\rm qp}^2}} \\ \pm \frac{\Delta_{\rm qp}}{\sqrt{\epsilon_L^2 - \Delta_{\rm qp}^2}} \frac{\Delta_{\rm qp}}{\sqrt{\epsilon_R^2 - \Delta_{\rm qp}^2}}\end{aligned} \tag{A11}$$

describing combinations of BCS densities of states. Both these functions and the lower integration limit depend on the self-consistent gap $\Delta_{\rm qp}$; however, since the integrand in Eq. (A10) is at least linear in the distribution function f, we can neglect the gap suppression by quasiparticles [see Eq. (44)] and approximate $\Delta_{\rm qp} \simeq \Delta$.

We note that the combinations of distribution functions in the last term of Eq. (A10) restricts to low energies only one of the energy integrals, while the other integral is logarithmically divergent. To isolate this divergence, we add and subtract the term obtained by setting $\omega_{ik} = 0$ in the denominator; more precisely, we define

$$P\frac{1}{\epsilon_L - \epsilon_R} = \frac{1}{2} \lim_{\omega\to 0^+} \frac{1}{\epsilon_L - \omega - \epsilon_R} + \frac{1}{\epsilon_L + \omega - \epsilon_R} \tag{A12}$$

and separate in $\delta E_i^{(1)} = \delta E_i^{(1),f} + \delta E_i^{(1),d}$ a finite term,

$$\begin{aligned}\delta E_i^{(1),f} = \frac{8E_J}{\pi^2\Delta} P \sum_{k\neq i} \int_\Delta^\infty d\epsilon_L \int_\Delta^\infty d\epsilon_R \\ \left[\left| \langle k| \sin\frac{\hat{\varphi}}{2} |i\rangle \right|^2 A_+(\epsilon_L,\epsilon_R) + \left| \langle k| \cos\frac{\hat{\varphi}}{2} |i\rangle \right|^2 A_-(\epsilon_L,\epsilon_R) \right] \\ \times f(\epsilon_L)(1-f(\epsilon_R)) \left[\frac{1}{\epsilon_L - \epsilon_R - \omega_{ik}} - \frac{1}{\epsilon_L - \epsilon_R} \right],\end{aligned} \tag{A13}$$

from a divergent one,

$$\begin{aligned}\delta E_i^{(1),d} = \frac{4E_J}{\pi^2\Delta} P \int_\Delta^\infty d\epsilon_L \int_\Delta^\infty d\epsilon_R \, \frac{f(\epsilon_L) - f(\epsilon_R)}{\epsilon_L - \epsilon_R} \\ \left[\frac{\epsilon_L}{\sqrt{\epsilon_L^2 - \Delta^2}} \frac{\epsilon_R}{\sqrt{\epsilon_R^2 - \Delta^2}} \right. \\ \left. - \langle i| \cos\hat{\varphi} |i\rangle \frac{\Delta}{\sqrt{\epsilon_L^2 - \Delta^2}} \frac{\Delta}{\sqrt{\epsilon_R^2 - \Delta^2}} \right].\end{aligned} \tag{A14}$$

To obtain this expression we used the identities

$$\sum_k \left| \langle k| \sin\frac{\hat{\varphi}}{2} |i\rangle \right|^2 + \left| \langle k| \cos\frac{\hat{\varphi}}{2} |i\rangle \right|^2 = 1 \tag{A15}$$

and

$$\sum_k \left| \langle k| \sin\frac{\hat{\varphi}}{2} |i\rangle \right|^2 - \left| \langle k| \cos\frac{\hat{\varphi}}{2} |i\rangle \right|^2 = -\langle i| \cos\hat{\varphi} |i\rangle \,. \tag{A16}$$

Equation (A13) for $\delta E_i^{(1),f}$ can be further simplified using the relations

$$\begin{aligned}&\epsilon_L\epsilon_R \left[\frac{1}{\epsilon_L - \epsilon_R - \omega_{ik}} - \frac{1}{\epsilon_L - \epsilon_R} \right] \\ &= \epsilon_L^2 \left[\frac{1}{\epsilon_L - \epsilon_R - \omega_{ik}} - \frac{1}{\epsilon_L - \epsilon_R} \right] - \frac{\epsilon_L \omega_{ik}}{\epsilon_L - \epsilon_R - \omega_{ik}} \\ &\simeq \Delta^2 \left\{ \left[\frac{1}{\epsilon_L - \epsilon_R - \omega_{ik}} - \frac{1}{\epsilon_L - \epsilon_R} \right] - \frac{\omega_{ik}/\Delta}{\epsilon_L - \epsilon_R - \omega_{ik}} \right\},\end{aligned} \tag{A17}$$

where the approximation is valid because the distribution function restricts the integral over ϵ_L to low energies above the gap. As discussed in Sec. II, the matrix elements of operators $e^{\pm i\hat{\varphi}/2}$ describe the transfer of a single charge. For this reason, for a low-lying level i the main contribution in the sum over states k comes either from levels with energy difference $\omega_{ik} \sim E_C \ll \Delta$ (when E_C is large compared to E_L, E_J), or from nearby levels (for small E_C). In both cases we have $\omega_{ik} \ll \Delta$, since at large energy differences the matrix elements quickly

decrease; this is evident, for example, in the expressions for the matrix elements in Sec. III. Then according to Eq. (A17) the term proportional to A_- is suppressed by the small parameter ω_{ik}/Δ in comparison to the leading term in A_+, and we can approximate $\delta E_i^{(1),f}$ as

$$\delta E_i^{(1),f} \simeq \frac{16E_J}{\pi^2\Delta} P \sum_{k\neq i} \int_\Delta^\infty d\epsilon_L \int_\Delta^\infty d\epsilon_R \left| \langle k| \sin\frac{\hat\varphi}{2} |i\rangle \right|^2 \frac{\Delta}{\sqrt{\epsilon_L^2-\Delta^2}} \frac{\Delta}{\sqrt{\epsilon_R^2-\Delta^2}} \times f(\epsilon_L)(1-f(\epsilon_R)) \left[\frac{1}{\epsilon_L-\epsilon_R-\omega_{ik}} - \frac{1}{\epsilon_L-\epsilon_R} \right]. \tag{A18}$$

Defining the function $F_{\rm qp}$ by

$$F_{\rm qp}(\omega) = \frac{16E_J}{\pi^2\Delta} P \int_\Delta^\infty d\epsilon_L \int_\Delta^\infty d\epsilon_R \frac{\Delta}{\sqrt{\epsilon_L^2-\Delta^2}} \frac{\Delta}{\sqrt{\epsilon_R^2-\Delta^2}} f(\epsilon_L)(1-f(\epsilon_R)) \left[\frac{1}{\epsilon_L-\epsilon_R-\omega} - \frac{1}{\epsilon_L-\epsilon_R} \right] \tag{A19}$$

we arrive at the expression for the quasiparticle correction to the energy $\delta E_{i,\rm qp}$ given in Eq. (46).

The treatment of the pair correction term $\delta E_i^{(2)}$ in Eq. (A6) is similar to the above one for $\delta E_i^{(1)}$. The pair correction is found by calculating the matrix element of $\hat H_T^p$ [Eq. (A3)] rather than $\hat H_T$ in Eq. (A8); we find

$$\delta E_i^{(2)} = \frac{4E_J}{\pi^2\Delta} P \sum_k \int_{\Delta_{\rm qp}}^\infty d\epsilon_L \int_{\Delta_{\rm qp}}^\infty d\epsilon_R \left[\left| \langle k| \sin\frac{\hat\varphi}{2} |i\rangle \right|^2 A_-(\epsilon_L,\epsilon_R) + \left| \langle k| \cos\frac{\hat\varphi}{2} |i\rangle \right|^2 A_+(\epsilon_L,\epsilon_R) \right] \times \left[\frac{f(\epsilon_L)f(\epsilon_R)}{\epsilon_L+\epsilon_R-\omega_{ik}} - \frac{(1-f(\epsilon_L))(1-f(\epsilon_R))}{\epsilon_L+\epsilon_R+\omega_{ik}} \right]. \tag{A20}$$

Note that in this expression there is a term independent of the distribution function, for which the approximation $\Delta_{\rm qp} \simeq \Delta$ is not applicable. Since $\epsilon_L+\epsilon_R \geq 2\Delta_{\rm qp}$, repeating the argument preceding Eq. (A18) we can neglect ω_{ik} in the denominator and use identities (A15)-(A16) to obtain

$$\delta E_i^{(2)} \simeq \frac{4E_J}{\pi^2\Delta} P \int_{\Delta_{\rm qp}}^\infty d\epsilon_L \int_{\Delta_{\rm qp}}^\infty d\epsilon_R \frac{f(\epsilon_L)+f(\epsilon_R)-1}{\epsilon_L+\epsilon_R} \left[\frac{\epsilon_L}{\sqrt{\epsilon_L^2-\Delta_{\rm qp}^2}} \frac{\epsilon_R}{\sqrt{\epsilon_R^2-\Delta_{\rm qp}^2}} + \langle i| \cos\hat\varphi |i\rangle \frac{\Delta_{\rm qp}}{\sqrt{\epsilon_L^2-\Delta_{\rm qp}^2}} \frac{\Delta_{\rm qp}}{\sqrt{\epsilon_R^2-\Delta_{\rm qp}^2}} \right]. \tag{A21}$$

Both in this expression and in Eq. (A14), the first term in square bracket does not depend on the level index i. Therefore, it leads to an unimportant common shift of all the levels which we neglect.[30] Keeping only the second term in each square brackets, we write

$$\delta E_i^{(1),d} + \delta E_i^{(2)} \approx \delta E_i^\Delta + \delta E_i^A, \tag{A22}$$

where, separating the terms independent of and proportional to the distribution function f, we have

$$\delta E_i^\Delta = -\frac{4E_J}{\pi^2\Delta} \langle i| \cos\hat\varphi |i\rangle P \int_{\Delta_{\rm qp}}^\infty d\epsilon_L \int_{\Delta_{\rm qp}}^\infty d\epsilon_R \frac{\Delta_{\rm qp}}{\sqrt{\epsilon_L^2-\Delta_{\rm qp}^2}} \frac{\Delta_{\rm qp}}{\sqrt{\epsilon_R^2-\Delta_{\rm qp}^2}} \frac{1}{\epsilon_L+\epsilon_R} \tag{A23}$$

and

$$\delta E_i^A = \frac{8E_J}{\pi^2\Delta} \langle i| \cos\hat\varphi |i\rangle\, P \int_\Delta^\infty d\epsilon_L \frac{\Delta}{\sqrt{\epsilon_L^2-\Delta^2}} f(\epsilon_L) \times \int_\Delta^\infty d\epsilon_R \frac{\Delta}{\sqrt{\epsilon_R^2-\Delta^2}} \left[\frac{1}{\epsilon_L+\epsilon_R} - \frac{1}{\epsilon_L-\epsilon_R} \right]. \tag{A24}$$

In both expressions the integrations can be performed analytically [using in Eq. (A24) the definition (A12)]. We obtain

$$\delta E_i^\Delta = -\frac{E_J}{\Delta} \Delta_{\rm qp} \langle i| \cos\hat\varphi |i\rangle \tag{A25}$$

and

$$\delta E_i^A = 2E_J f(\Delta) \langle i| \cos\hat\varphi |i\rangle\,. \tag{A26}$$

Finally, using Eqs. (23), (44), and (A7) we arrive at

$$\delta E_i^\Delta + \delta E_i^A + \delta E_i^{(3)} = E_J \left(x_{\rm qp} + 2x_{\rm qp}^{\rm A} \right) \langle i| \cos\hat\varphi |i\rangle\,, \tag{A27}$$

which is the correction $\delta E_{i,E_J}$ in Eq. (45). This result, together with Eqs. (A18)-(A19), concludes the derivation of the formulas presented in Sec. II C.

Appendix B: Gate-dependent energy splitting in the transmon

The transmon low-energy spectrum is characterized by well separated [by the plasma frequency ω_p, Eq. (56)] and nearly degenerate levels whose energies, as shown in Fig. 2, vary periodically with the gate voltage n_g. Here we derive the asymptotic expression (valid at large E_J/E_C) for the energy splitting between the nearly degenerate levels. We consider first the two lowest energy states and then generalize the result to higher energies.

Using the notation of Sec. II, the transmon Hamiltonian is

$$\hat H_\varphi = 4E_C \left(\hat N - n_g \right)^2 - E_J \left(1+\cos\hat\varphi \right). \tag{B1}$$

Its eigengstates can be written exactly in terms of Mathieu functions.[2] However, since $E_J \gg E_C$ a tight-binding

approach[31] can be used in which the two lowest (even and odd) eigenstates Ψ^e and Ψ^o are given by sums of localized wavefunctions,

$$\Psi^e(\varphi; n_g) = e^{in_g\varphi}\frac{1}{\sqrt{L}}\sum_j \psi(\varphi - 2\pi j)e^{-in_g 2\pi j}, \quad \text{(B2)}$$

$$\Psi^o(\varphi; n_g) = e^{in_g\varphi}\frac{1}{\sqrt{L}}\sum_j \psi(\varphi - 2\pi j)e^{-in_g 2\pi j}e^{-i\pi j},$$

where $L \gg 1$ is the number of sites, labeled with index j, and ψ is the ground state of the Hamiltonian

$$\hat{H} = 4E_C\hat{N}^2 + V(\hat{\varphi}) \quad \text{(B3)}$$

with

$$V(\varphi) = \begin{cases} -E_J(1+\cos\varphi), & |\varphi| < \pi \\ 0, & |\varphi| > \pi \end{cases}. \quad \text{(B4)}$$

This potential is such that $\sum_j V(\varphi - 2\pi j) = -E_J(1+\cos\varphi)$. Note that the even (odd) state is a linear combination of even (odd) charge eigenstates, as can be shown by considering the overlap of $\Psi^{e(o)}$ with the charge eigenstate $e^{in\varphi/2}$ for arbitrary integer n [in Eq. (B2) what distinguish the odd state from the even one is the last exponential in the expression for Ψ^o, which changes the sign of the localized wavefunction at odd sites j].

The energy difference ω_{eo} between the two states is

$$\omega_{eo} = \langle\Psi^o|\hat{H}_\varphi|\Psi^o\rangle - \langle\Psi^e|\hat{H}_\varphi|\Psi^e\rangle\,. \quad \text{(B5)}$$

Using Eq. (B2), the contributions to ω_{eo} due to products of wavefunctions ψ localized at the same site cancel. The leading contribution to ω_{eo} originates from products of wavefunctions localized at nearby sites,

$$\omega_{eo} = \epsilon_0\cos(2\pi n_g) \quad \text{(B6)}$$

with

$$\epsilon_0 = -4\int d\varphi\,\psi(\varphi)\psi(\varphi - 2\pi)V(\varphi)\,. \quad \text{(B7)}$$

To estimate the above integral, the behavior of the wavefunction ψ near $\varphi = \pi$ is needed; in this region a good approximation is given by the semiclassical wavefunction[32]

$$\psi(\varphi) \simeq \begin{cases} \frac{C_0}{2\sqrt{p(\varphi)}}\exp\left[-\int_a^\varphi d\phi\,p(\phi)\right], & a < \varphi < \pi \\ A_0\exp\left[-\sqrt{\frac{E_J}{2E_C}\left(1-\frac{\omega_p}{4E_C}\right)}(\varphi-\pi)\right], & \varphi > \pi \end{cases} \quad \text{(B8)}$$

where C_0 and A_0 are constants,

$$p(\varphi) = \sqrt{\frac{E_J}{4E_C}}\sqrt{1 - \frac{\omega_p}{2E_J} - \cos\varphi}\,, \quad \text{(B9)}$$

and a is the classical turning point defined by $p(a) = 0$. The constant C_0 is determined by the normalization condition of the wavefunction, and A_0 then follows from continuity of the wavefunction. For states with large quantum number the semiclassical approximation can be used also in the classically accessible region $|\varphi| < a$; the corresponding estimate for the normalization constant, which we indicate with C_∞, is $C_\infty = \sqrt{\omega_p/4E_C\pi}$ – see Ref. 32. Here we are interested in the ground state (and more generally in low-lying states), for which C_∞ is known to underestimate the normalization factor.[24,33] To evaluate C_0 we note that for $|\varphi| \ll \pi$ the potential $V(\varphi)$ in Eq. (B4) is well approximated by that of the harmonic oscillator; therefore the semiclassical wavefunction (B8) should match the normalized wavefunction of the harmonic oscillator given in Eq. (87) (with $\varphi_m = 0$) in the region $a \ll \varphi \ll \pi$. Indeed, in this region we expand the cosine in Eq. (B9) and rescale variables ($\phi = \tilde{\phi}\sqrt{\omega_p/E_J}$) to find

$$\begin{aligned}\int_a^\varphi d\phi\,p(\phi) &\simeq \int_1^{\tilde{\varphi}} d\tilde{\phi}\sqrt{\tilde{\phi}^2 - 1} \quad \text{(B10)}\\ &= \frac{1}{2}\left[\tilde{\varphi}\sqrt{\tilde{\varphi}^2-1} - \ln\left(\tilde{\varphi} + \sqrt{\tilde{\varphi}^2-1}\right)\right]\\ &\simeq \frac{1}{2}\frac{E_J}{\omega_p}\varphi^2 - \frac{1}{4} - \frac{1}{2}\ln\left(2\varphi\sqrt{E_J/\omega_p}\right).\end{aligned}$$

Using this expression, and $p(\varphi) \simeq \varphi\sqrt{E_J/8E_C}$ in the denominator, Eq. (B8) becomes

$$\psi(\varphi) \simeq C_0\frac{e^{1/4}}{\sqrt{2}}\left(\frac{8E_C}{E_J}\right)^{1/8} e^{-\varphi^2 E_J/2\omega_p}. \quad \text{(B11)}$$

This function matches Eq. (87) by setting

$$C_0 = \sqrt{\frac{\omega_p}{4E_C}}(\pi e)^{-1/4} = C_\infty\left(\frac{\pi}{e}\right)^{1/4}. \quad \text{(B12)}$$

The last form shows that the correct normalization factor is larger than the usual semiclassical estimate.

Having found the normalization constant, we now consider the wavefunction in the region near $\varphi = \pi$. There we can further simplify Eq. (B8) as follows: we rewrite the integral in the exponential in the first line of Eq. (B8) as

$$\int_a^\varphi d\phi\,p(\phi) = \int_a^\pi d\phi\,p(\phi) - \int_\varphi^\pi d\phi\,p(\phi)\,. \quad \text{(B13)}$$

Then the first integral on the right hand side is

$$\int_a^\pi d\phi\,p(\phi) = \sqrt{\frac{2E_J}{E_C}}\left[E(k) - (1-k^2)K(k)\right], \quad \text{(B14)}$$

where E and K denote the complete elliptic integrals with modulus k, which has the value

$$k^2 \equiv 1 - k'^2 = 1 - \frac{\omega_p}{4E_J}\,. \quad \text{(B15)}$$

Here we are interested in the limit $k \to 1$, in which the complete elliptic integrals behave as

$$\begin{aligned}E(k) &\simeq 1 + \frac{1}{2}k'^2\left(\ln\frac{4}{k'} - \frac{1}{2}\right),\\ K(k) &\simeq \ln\frac{4}{k'}\,.\end{aligned} \quad \text{(B16)}$$

The last integral in Eq. (B13) can be approximated as

$$\int_{\varphi}^{\pi} d\phi\, p(\phi) \simeq \sqrt{\frac{E_J}{2E_C}}\Big[\sqrt{1-\frac{\omega_p}{4E_J}}(\pi-\varphi) - \frac{(\pi-\varphi)^3}{24\sqrt{1-\omega_p/4E_J}}\Big]. \tag{B17}$$

Substituting Eqs. (B13)-(B17) into Eq. (B8), using $p(\pi) \simeq \sqrt{E_J/2E_C}$ in the square root in the denominator of the first line, and requiring continuity of the wavefunction, we arrive at

$$\psi(\varphi) = \begin{cases} A_0 \exp\Big\{ -\sqrt{\frac{E_J}{2E_C}}\Big[\sqrt{1-\frac{\omega_p}{4E_J}}(\varphi-\pi),\ \varphi \lesssim \pi \\ \qquad\qquad -\frac{(\varphi-\pi)^3}{24\sqrt{1-\omega_p/4E_J}}\Big]\Big\} \\ A_0 \exp\Big[-\sqrt{\frac{E_J}{2E_C}}\sqrt{1-\frac{\omega_p}{4E_J}}(\varphi-\pi)\Big], \quad \varphi > \pi \end{cases} \tag{B18}$$

with

$$A_0 = \frac{1}{(2\pi)^{1/4}}\left(\frac{8E_J}{E_C}\right)^{1/8} e^{-\sqrt{2E_J/E_C}}\,. \tag{B19}$$

The wavefunction near $\varphi = -\pi$ can be obtained by substituting $\varphi \to -\varphi$ in Eq. (B18). We can now proceed with the calculation of the integral in Eq. (B7). Using Eqs. (B4) and (B18), expanding the potential for $\varphi \le \pi$, and changing the integration variable ($\varphi \to \pi - \varphi$) we find

$$\begin{aligned}\epsilon_0 &\simeq 2E_J A_0^2 \int_0 d\varphi\, \varphi^2 \exp\left[-\sqrt{\frac{E_J}{2E_C}}\,\frac{\varphi^3}{24\sqrt{1-\omega_p/4E_J}}\right] \\ &\simeq 8\omega_p A_0^2 = 4\sqrt{\frac{2}{\pi}}\omega_p \left(\frac{8E_J}{E_C}\right)^{1/4} e^{-\sqrt{8E_J/E_C}}\end{aligned} \tag{B20}$$

where, going from the first to the second line, we neglect the subleading correction originating from the denominator in the argument of the exponential. The final expression for ϵ_0 agrees with the known asymptotic formula,[2,14,24] thus validating our approach.

The above result can be generalized to calculate the splitting between nearly degenerate even/odd states of approximate energy $n\omega_p$ above the ground state by letting $\omega_p \to \omega_p(2n+1)$ in Eqs. (B8)-(B9) and those that follow [this replacement is appropriate so long as $\omega_p(n+1/2) \ll 2E_J$]. Matching the semiclassical wavefunction to the excited eigenstates of the harmonic oscillator, we find that the normalization coefficient depends on n,

$$C_n = \sqrt{\frac{\omega_p}{4E_C}}\left(\frac{2}{\pi e}\right)^{1/4}\left(\frac{n+1/2}{e}\right)^{n/2}\left(\frac{\sqrt{n+1/2}}{n!}\right)^{1/2}. \tag{B21}$$

Note that C_n approaches C_∞ as n grows. Repeating the above calculation, we find the energy splitting

$$\epsilon_n = \epsilon_0(-1)^n \frac{2^{2n}}{n!}\left(\frac{8E_J}{E_C}\right)^{n/2}, \tag{B22}$$

also in agreement with the expression in the literature.

Appendix C: Rate of parity switching induced by quasiparticles in the transmon

The spectrum of the transmon, as described in Appendix B, comprises both well separated and nearly degenerate levels of opposite parity (see also Fig. 2). The leading contribution to the transition rate between states of different parity separated in energy by (approximately) the plasma frequency is given by Eq. (55) with $\varphi_0 = 0$ and is independent of n_g. Here we consider the quasiparticle-induced transitions between the nearly degenerate states Ψ^e and Ψ^o. We first consider a single-junction transmon to show explicitly that the rate depends on n_g and is exponentially small. Next we study the experimentally relevant case of a split transmon; its rate is qualitatively different, not displaying such exponential smallness.

1. Single-junction transmon

According to Eq. (32), the quasiparticle transition rate $\Gamma_{o\to e}$ between states Ψ^o and Ψ^e can be written as

$$\Gamma_{o\to e} = \left|\langle\Psi^e|\sin\frac{\hat\varphi}{2}|\Psi^o\rangle\right|^2 S_{\rm qp}\left(\omega_{eo}\right). \tag{C1}$$

This rate depends on the gate voltage n_g via the states in the matrix element as well as via their energy difference ω_{eo}, see Eq. (B6). For the matrix element we use Eq. (B2) to find

$$\left|\langle\Psi^e|\sin\frac{\hat\varphi}{2}|\Psi^o\rangle\right| \simeq |\sin(2\pi n_g)|\, s\,, \tag{C2}$$

where

$$s = 2\left|\int d\varphi\, \psi(\varphi)\psi(\varphi-2\pi)\sin\frac{\varphi}{2}\right|. \tag{C3}$$

The matrix element in Eq. (C2) vanishes at half integer values of n_g, as in the case of the Cooper pair box [see Eq. (83)]. In fact, the vanishing holds at arbitrary ratio E_J/E_C, as can be shown using the symmetry properties of Mathieu functions. For example, at $n_g = 0,\ 1/2$ the two lowest eigenstates of the transmon Hamiltonian, Eq. (B1), can be written in the charge basis as[34]

$$\begin{aligned}|\Psi^e\rangle &= \sum_{m=0}^{\infty} A^{(0)}_{2m}\Big[|2m\rangle + |-2m\rangle\Big], \\ |\Psi^o\rangle &= \sum_{m=0}^{\infty} A^{(1)}_{2m+1}\Big[|2m+1\rangle + |-(2m+1)\rangle\Big],\end{aligned} \tag{C4}$$

and

$$|\Psi^e\rangle = \sum_{m=0}^{\infty} A^{(1)}_{2m+1}\Big[|2m+2\rangle + |-2m\rangle\Big],$$
$$|\Psi^o\rangle = \sum_{m=0}^{\infty} A^{(0)}_{2m}\Big[|2m+1\rangle + |-2m+1\rangle\Big], \tag{C5}$$

respectively, where the coefficients $A^{(0)}_{2m}$, $A^{(1)}_{2m+1}$ depend on the ratio E_J/E_C.[35] Using the charge basis representation of $\sin\hat{\varphi}/2$ in Eq. (82) it is easy to check the vanishing of its matrix element between the above states for both values of n_g.

In the transmon limit $E_J/E_C \gg 1$ under consideration, the product of wavefunctions localized at the same site does not contribute to the matrix element in Eq. (C2): the intrawell integral vanishes because $\psi^2(\varphi)$ is a symmetric function (ψ being the ground state of a symmetric potential) which is multiplied by the antisymmetric function $\sin\varphi/2$; the vanishing of the intrawell term has thus he same origin of the vanishing of the matrix element for a weakly anharmonic qubit at zero phase bias, see Eq. (53) with $n = m$ and $\varphi_0 = 0$. To estimate the interwell contribution s in Eq. (C3), we use Eq. (B18) and that near $\varphi = \pi$ we have $\sin\varphi/2 \simeq 1$. After changing integration variable ($\varphi \to \pi - \varphi$) we arrive at

$$s \simeq 4A_0^2 \int_0 d\varphi\, \exp\left[-\sqrt{\frac{E_J}{2E_C}}\,\frac{\varphi^3}{24\sqrt{1-\omega_p/4E_J}}\right]$$
$$\simeq D\left(\frac{E_C}{E_J}\right)^{1/6}\frac{\epsilon_0}{\omega_p}\,, \tag{C6}$$

where (with Γ denoting here the gamma function)

$$D = 2^{1/6}3^{-2/3}\Gamma\left(\frac{1}{3}\right) \approx 1.45\,. \tag{C7}$$

Due to the factor ϵ_0 in Eq. (C6), the transition rate in Eq. (C1) is indeed exponentially small. Turning now to the factor $S_{\rm qp}$ in Eq. (C1), we note that its argument, ω_{eo}, is usually small due to its exponential suppression at large E_J/E_C, see Eq. (B20). Therefore the "high frequency" condition $\omega_{eo} \gg \delta E$ (with δE the characteristic quasiparticle energy) is in general not satisfied and use of Eq. (41) expressing $S_{\rm qp}$ in terms of the quasiparticle density is not appropriate. In thermal equilibrium, one can use Eq. (35) for arbitrary ratio ω_{eo}/T. Assuming $\epsilon_0 \ll T$, using Eq. (17), Eq. (35), and the above results, we rewrite Eq. (C1) as

$$\Gamma_{o\to e} = \frac{16E_J}{\pi}e^{-\Delta/T}\left[\ln\frac{4T}{|\epsilon_0\cos(2\pi n_g)|} - \gamma_E\right]$$
$$\times\left(\frac{E_C}{E_J}\right)^{1/3}\left(D\frac{\epsilon_0}{\omega_p}\right)^2\sin^2(2\pi n_g)\,. \tag{C8}$$

Generalization of this result to the transition rate $\Gamma^{(n)}_{o\to e}$ between nearly degenerate states of higher energy is obtained by the substitution $\epsilon_0 \to \epsilon_n$. Except at the degeneracy points $n_g = 1/4,\, 3/4$ (where this expression diverges), we can estimate the rate in order of magnitude by assuming $\sin(2\pi n_g),\ \cos(2\pi n_g) \approx 1$. For low-lying states, this estimate shows that the rate $\Gamma^{(n)}_{o\to e}$ is small compared to the rate $\Gamma_{1\to 0}$ determining the relaxation time of the transmon [see Eq. (55)]. This smallness is due to the exponentially suppressed $o \to e$ matrix element, Eq. (C6), as function of the ratio E_J/E_C, in comparison with the weak power-law suppression of the $1 \to 0$ matrix element as given by Eq. (53) with $\varphi_0 = 0$, $m = 1$, and $n = 0$. The relationship between the two rates is qualitatively different in the split transmon, as we discuss next.

2. Split transmon

The above calculation of the even/odd transition rate in the single junction transmon can be easily modified to yield the rate for a split transmon. As discussed in Sec. V A, the effective Hamiltonian and therefore the form of the eigenstates are the same in the single and split transmon. The difference between the two cases arises in the evaluation of the matrix elements pertaining to each junction [cf. Eq. (125)]. For the even/odd matrix element we find

$$\left|\langle\Psi^e|\sin\frac{\hat{\varphi}_j}{2}|\Psi^o\rangle\right|^2 \simeq \frac{1-\cos(\pi f \pm \vartheta)}{2}\,, \tag{C9}$$

where the upper (lower) sign applies to junction $j = 1$ ($j = 0$), f is defined in Eq. (88) and ϑ in Eq. (118). In contrast with the single-junction transmon case considered above, here the matrix element is dominated by the intrawell contribution having the same form of Eq. (53) at $n = m = 0$ and finite phase bias $\pi f \pm \vartheta$. Substituting Eq. (C9) into Eq. (109) and assuming thermal equilibrium quasiparticles [cf. Eq. (35)] we obtain

$$\Gamma_{o\to e} = \frac{8(E_{J0}+E_{J1})}{\pi}e^{-\Delta/T}e^{\omega_{eo}/2T}K_0\left(\frac{|\omega_{eo}|}{2T}\right)$$
$$\left(1-\frac{\omega_p^2(f)}{\omega_p^2(0)}\right) \tag{C10}$$

with $\omega_p(f)$ given in Eq. (120) and ω_{eo} in Eq. (B6). As before, the rate $\Gamma^{(n)}_{o\to e}$ of transitions between nearly degenerate levels of higher energy is obtained upon the substitution $\omega_{eo} \to \epsilon_n\sin(2\pi n_g)$ in Eq. (C10). Note that the rate vanishes at integer multiples of the flux quantum; at those values of flux, exponentially small contributions to the matrix element analogous to those calculated above should be included. At non-integer values of reduced flux f, Eq. (C10) should be compared with the transition rate

between qubit states induced by thermal quasiparticles,

$$\Gamma_{1\to 0} = \frac{8(E_{J0}+E_{J1})}{\pi} e^{-\Delta/T} e^{\omega_p(f)/2T} K_0\left(\frac{|\omega_p(f)|}{2T}\right) \frac{E_C}{\omega_p(f)}\left(1+\frac{\omega_p^2(f)}{\omega_p^2(0)}\right), \tag{C11}$$

obtained using Eq. (125). The ratio between these two quantities,

$$\frac{\Gamma_{o\to e}}{\Gamma_{1\to 0}} = \frac{e^{\omega_{eo}/2T} K_0\left(\frac{|\omega_{eo}|}{2T}\right)}{e^{\omega_p(f)/2T} K_0\left(\frac{|\omega_p(f)|}{2T}\right)} \frac{\omega_p(f)}{E_C} \frac{\omega_p^2(0)-\omega_p^2(f)}{\omega_p^2(0)+\omega_p^2(f)} \tag{C12}$$

depends on temperature through the first factor on the right hand side. Experimentally, measurements for the rate are performed near $n_g = 1/2$, so that the relevant even/odd frequencies are $\omega_{eo} \sim \epsilon_0,\ \epsilon_1$; they are generally 2-3 orders of magnitude smaller than $\omega_p(f)$ ($\sim 2\pi \times 4$ GHz), while the latter is usually larger than twice the temperature ($T \sim 20-200$ mK). Under these conditions, the first factor in Eq. (C12) can be approximated, in order of magnitude, by 5 to 10. The last factor in Eq. (C12) varies between 0 at $f = 0$ and 1 at $f = 1/2$; as flux is used to suppress the qubit frequency from its maximum value ($\gtrsim 10$ GHz), we can approximate the last factor by 1/2. Finally, the central factor can be rewritten as $\sqrt{8E_J(f)/E_C}$; since $E_J(f)/E_C$ usually is varied between 10 and 30, we arrive at the order-of-magnitude estimate

$$\frac{\Gamma_{o\to e}}{\Gamma_{1\to 0}} \sim 20-80 \tag{C13}$$

in the experimentally relevant ranges of parameters. This is an example of the more general statement that, except close to integer values of f, the even/odd transition rate in a split transmon is faster than its decay rate. This result is qualitatively in agreement with experimental bounds for the even/odd transition rate in split transmons.[36,37]

Appendix D: Matrix elements for the harmonic oscillator

In this Appendix we present analytic expression for the matrix elements of $\sin\hat{\varphi}/2$ between harmonic oscillator states $|n\rangle$ and $|m\rangle$. Let us introduce the displacement operator

$$\hat{D}(\mu) = e^{\mu\hat{a}^\dagger - \mu^*\hat{a}}, \tag{D1}$$

where $\hat{a}$ ($\hat{a}^\dagger$) is the harmonic oscillator annihilation (creation) operator. The matrix elements of $\hat{D}$ are[38]

$$\langle m|\hat{D}(\mu)|n\rangle = \begin{cases} e^{-|\mu|^2/2}\sqrt{\frac{m!}{n!}}(-\mu^*)^{n-m} L_m^{(n-m)}\left(|\mu|^2\right), & m \le n \\ e^{-|\mu|^2/2}\sqrt{\frac{n!}{m!}}(\mu)^{m-n} L_n^{(m-n)}\left(|\mu|^2\right), & m \ge n \end{cases} \tag{D2}$$

where $L_n^{(\alpha)}$ are the generalized Laguerre polynomials. Since the position operator is $\hat{\varphi} = \ell(\hat{a}+\hat{a}^\dagger)/\sqrt{2}$, where $\ell = 1/\sqrt{m\omega}$ is the oscillator length for an oscillator of mass m and frequency ω, we can write

$$e^{i\hat{\varphi}/2} = \hat{D}\left(\frac{i\ell}{2\sqrt{2}}\right). \tag{D3}$$

Note that for the harmonic oscillator described by Eq. (50) we have

$$\ell = 2\sqrt{2}\sqrt{\frac{E_C}{\omega_{10}}}. \tag{D4}$$

To allow for fluctuations around a finite phase, we shift $\hat{\varphi} \to \varphi_0 + \hat{\varphi}$ in the argument of sine and rewrite the resulting expression in terms of exponentials,

$$\sin\frac{\varphi_0+\hat{\varphi}}{2} = \frac{1}{2i}\left(e^{i\varphi_0/2}e^{i\hat{\varphi}/2} - e^{-i\varphi_0/2}e^{-i\hat{\varphi}/2}\right). \tag{D5}$$

Then using Eqs. (D2)-(D3) we find for $m \le n$

$$\langle m|\sin\frac{\varphi_0+\hat{\varphi}}{2}|n\rangle = e^{-\ell^2/16}\sqrt{\frac{m!}{n!}}\left(\frac{\ell}{2\sqrt{2}}\right)^{n-m} \times L_m^{(n-m)}\left(\frac{\ell^2}{8}\right)\sin\frac{\varphi_0+\pi(n-m)}{2}. \tag{D6}$$

The matrix element for $m \ge n$ is obtained by exchanging $n \leftrightarrow m$ in the right hand side. Equation (53) can be obtained from Eq. (D6) by Taylor expansion for small ℓ, which for the Laguerre polynomials gives

$$L_m^{(\alpha)}(x) = \frac{(m+\alpha)!}{m!\alpha!} - \frac{(m+\alpha)!}{(m-1)!(\alpha+1)!}x + \mathcal{O}(x^2). \tag{D7}$$

Equation (58) follows from Eq. (D6) with $m = 0$ using $L_0^{(\alpha)}(x) = 1$.

Using Eq. (D2) we can also find the expectation value of the operator $\cos\hat{\varphi}$. After shifting the phase variable as done above and since the expectation value of sine vanishes by symmetry, we find

$$\langle n|\cos\left(\varphi_0+\hat{\varphi}\right)|n\rangle = \cos\varphi_0\langle n|\cos\hat{\varphi}|n\rangle. \tag{D8}$$

Writing the cosine in exponential form, using $e^{i\hat{\varphi}} = \hat{D}\left(i\ell/\sqrt{2}\right)$ we arrive at

$$\langle n|\cos\left(\varphi_0+\hat{\varphi}\right)|n\rangle = \cos\varphi_0\, e^{-\ell^2/4} L_n^{(0)}\left(\frac{\ell^2}{2}\right). \tag{D9}$$

Appendix E: Matrix elements for the transmon

Here we want to show that corrections to Eq. (53) for the transmon ($\varphi_0 = 0$) are of cubic order in E_C/ω_p, as claimed in the text following that equation. The transmon Hamiltonian is given by Eq. (B1) and we neglect exponentially small corrections by setting $n_g = 0$ (see Ref. 2 and Appendices B and C). Numbering the eigenstates $|\psi_n\rangle$ starting with $n = 0$ for the ground state, even (odd) numbered states are even (odd) functions of φ, due to the symmetry of the potential energy. Since $\sin\varphi/2$ is an odd function, the matrix element between states of the same parity vanishes,

$$\langle\psi_{n\pm 2j}|\sin\frac{\hat\varphi}{2}|\psi_n\rangle = 0\,, \qquad j = 0, 1, 2, \ldots \tag{E1}$$

Due to the smallness of the charging energy, $E_C \ll E_J$, as a first approximation we can expand the Josephson energy in Eq. (B1) up to the fourth order in φ. In terms of creation/annihilation operators (cf. Appendix D – note that in the present case $\ell = 2\sqrt{2}\sqrt{E_C/\omega_p} \ll 1$), the approximate transmon Hamiltonian is

$$\hat H = \hat H_0 + \delta\hat H\,, \tag{E2}$$

$$\hat H_0 = \omega_p\left(\hat a^\dagger\hat a + \frac{1}{2}\right), \tag{E3}$$

$$\delta\hat H = -\frac{E_C}{12}\left(a + a^\dagger\right)^4. \tag{E4}$$

To first order in E_C/ω_p, expressed in terms of harmonic oscillator states the transmon eigenstates are therefore

$$|\psi_n\rangle = |n\rangle + |\delta\psi_n\rangle\,, \tag{E5}$$

$$|\delta\psi_n\rangle = -\sum_{j\neq n}|j\rangle\frac{\langle j|\delta\hat H|n\rangle}{E_j - E_n}\,, \qquad E_n = \omega_p\left(n + \frac{1}{2}\right),$$

and including the first anharmonic corrections to the eigenstates the matrix elements are

$$\begin{aligned}\langle\psi_m|\sin\frac{\hat\varphi}{2}|\psi_n\rangle \simeq \langle m|\sin\frac{\hat\varphi}{2}|n\rangle + \langle m|\sin\frac{\hat\varphi}{2}|\delta\psi_n\rangle \\ +\langle\delta\psi_m|\sin\frac{\hat\varphi}{2}|n\rangle\,.\end{aligned} \tag{E6}$$

Using Eq. (D6), we find that the leading contribution to the first term on the right hand side is

$$\langle n \pm (2j+1)|\sin\frac{\hat\varphi}{2}|n\rangle \propto \left(\frac{E_C}{\omega_p}\right)^{j+1/2}, \quad j = 0, 1, 2, \ldots \tag{E7}$$

Since we are interested in calculating the square of the matrix elements up to second order in E_C/ω_p, we can neglect transitions with $j \geq 1$. For $j = 0$, using Eq. (D6) at next to leading order we find

$$\begin{aligned}\langle n \pm 1|\sin\frac{\hat\varphi}{2}|n\rangle \simeq \sqrt{\left(n + \frac{1}{2} \pm \frac{1}{2}\right)\frac{E_C}{\omega_p}} \\ \times\left[1 - \frac{1}{2}\left(n + \frac{1}{2} \pm \frac{1}{2}\right)\frac{E_C}{\omega_p} + \mathcal{O}\left(\frac{E_C}{\omega_p}\right)^2\right].\end{aligned} \tag{E8}$$

Consider now the case $m = n - 1$ in Eq. (E6). Using Eqs. (E4), (E5), and the leading term in Eq. (E8), the central term in the right hand side is approximately

$$\begin{aligned}\langle n-1|\sin\frac{\hat\varphi}{2}|\delta\psi_n\rangle &\simeq -\langle n-1|\sin\frac{\varphi}{2}|n-2\rangle\frac{\langle n-2|\delta\hat H|n\rangle}{E_{n-2} - E_n} \\ &\simeq -\frac{1}{24}\left(\frac{E_C}{\omega_p}\right)^{3/2}\sqrt{n-1}\langle n-2|\left(a + a^\dagger\right)^4|n\rangle\,.\end{aligned} \tag{E9}$$

To calculate the last factor we note that

$$\begin{aligned}\left(a + a^\dagger\right)^2|n\rangle = \sqrt{n(n-1)}|n-2\rangle + (2n+1)|n\rangle \\ +\sqrt{(n+1)(n+2)}|n+2\rangle.\end{aligned} \tag{E10}$$

Shifting $n \to n - 2$ and taking the scalar product we arrive at

$$\langle n-2|\left(a + a^\dagger\right)^4|n\rangle = 4\sqrt{n(n-1)}\left(n - \frac{1}{2}\right), \tag{E11}$$

and substituting this expression into Eq. (E9) we obtain

$$\langle n-1|\sin\frac{\hat\varphi}{2}|\delta\psi_n\rangle = -\frac{1}{6}\left(\frac{E_C}{\omega_p}\right)^{3/2}\sqrt{n}(n-1)\left(n - \frac{1}{2}\right). \tag{E12}$$

Proceeding as above we also find

$$\langle\delta\psi_{n-1}|\sin\frac{\hat\varphi}{2}|n\rangle = \frac{1}{6}\left(\frac{E_C}{\omega_p}\right)^{3/2}\sqrt{n}(n+1)\left(n + \frac{1}{2}\right). \tag{E13}$$

Finally, substitution of Eqs. (E8), (E12), and (E13) into Eq. (E6) gives

$$\langle\psi_{n-1}|\sin\frac{\hat\varphi}{2}|\psi_n\rangle = \sqrt{n\frac{E_C}{\omega_p}} + \mathcal{O}\left(\frac{E_C}{\omega_p}\right)^{5/2}. \tag{E14}$$

Repeating the above calculations for the case $m = n+1$ and using Eq. (E7) we conclude that the square of the matrix element is

$$\begin{aligned}\left|\langle\psi_m|\sin\frac{\hat\varphi}{2}|\psi_n\rangle\right|^2 = \frac{E_C}{\omega_p}\left[n\delta_{m,n-1} + (n+1)\delta_{m,n+1}\right] \\ +\mathcal{O}\left(\frac{E_C}{\omega_p}\right)^3.\end{aligned} \tag{E15}$$

Appendix F: Multi-junction Hamiltonian

The aim of this Appendix is to derive the Hamiltonian for a multi-junction system starting from the Lagrangian, Eq. (105). We consider a loop of $M+1$ junctions and assume M of them, denoted by index j with $j = 1, \ldots, M$, to be identical, so that their capacitances and Josephson energies are, respectively, $C_j = C_1$ and $E_{Jj} = E_{J1}$ for $1 \leq j \leq M$. These M junctions will be referred to as the

array junctions to distinguish them from the $j=0$ junction, whose capacitance C_0 and Josephson energy E_{J0} can differ from those of the array junctions.

While the system comprises $M+1$ junctions, there are only M independent degrees of freedom, due to the flux quantization constraint, Eq. (104). Using that equation to eliminate the phase φ_0, the Lagrangian is

$$\mathcal{L}_{\{\varphi\}} = \frac{1}{2}\frac{C_0}{(2e)^2}\left(\sum_{j=1}^{M}\dot{\varphi}_j\right)^2 + \frac{1}{2}\frac{C_1}{(2e)^2}\sum_{j=1}^{M}\dot{\varphi}_j^2 \qquad \text{(F1)}$$
$$+E_{J0}\cos\left(\sum_{j=1}^{M}\varphi_j - 2\pi\Phi_e/\Phi_0\right) + E_{J1}\sum_{j=1}^{M}\cos\varphi_j\,.$$

We introduce a new set $\{\phi\}$ of M independent variables

$$\phi \;= \sum_{j=1}^{M}\varphi_j\,, \qquad \text{(F2)}$$

$$\phi_k \;= \varphi_k - \alpha\sum_{l=1}^{M-1}\varphi_l + \frac{\varphi_M}{\sqrt{M}}\,, \quad k=1,\ldots,M-1\,, \qquad \text{(F3)}$$

where

$$\alpha = \left(1+\frac{1}{\sqrt{M}}\right)\frac{1}{M-1}. \qquad \text{(F4)}$$

The inverse transformation is given by

$$\varphi_k \;= \phi_k - \alpha\sum_{l=1}^{M-1}\phi_l + \frac{1}{M}\phi\,, \qquad k=1,\ldots,M-1,$$
$$\varphi_M \;= \frac{1}{\sqrt{M}}\sum_{l=1}^{M-1}\phi_l + \frac{1}{M}\phi\,. \qquad \text{(F5)}$$

In terms of the M variables ϕ, ϕ_k $(k=1,\ldots,M-1)$ the Lagrangian is

$$\mathcal{L}_{\{\phi\}} = \frac{1}{8e^2}\left(C_0+\frac{C_1}{M}\right)\dot{\phi}^2 + \frac{1}{8e^2}C_1\sum_{k=1}^{M-1}\dot{\phi}_k^2 - U(\{\phi\}) \qquad \text{(F6)}$$

with potential energy

$$\begin{aligned} U(\{\phi\}) = &- E_{J0}\cos\left(\phi - 2\pi\Phi_e/\Phi_0\right) \\ &- E_{J1}\sum_{k=1}^{M-1}\cos\left(\phi_k - \alpha\sum_{l=1}^{M-1}\phi_l + \frac{\phi}{M}\right) \\ &- E_{J1}\cos\left(\frac{1}{\sqrt{M}}\sum_{l=1}^{M-1}\phi_l + \frac{\phi}{M}\right). \end{aligned} \qquad \text{(F7)}$$

Introducing the M conjugate variables $N = \partial\mathcal{L}_\phi/\partial\dot{\phi}$ and $N_k = \partial\mathcal{L}_\phi/\partial\dot{\phi}_k$ $(k=1,\ldots,M-1)$, the Hamiltonian is

$$\begin{aligned} H_{\{\phi\}} &= N\dot{\phi} + \sum_{k=1}^{M-1}N_k\dot{\phi}_k - \mathcal{L}_{\{\phi\}} \\ &= 4E_C N^2 + 4E_{C1}\sum_{k=1}^{M-1}N_k^2 + U(\{\phi\}), \end{aligned} \qquad \text{(F8)}$$

where

$$E_C = \frac{e^2}{2(C_0+C_1/M)}\,, \qquad E_{C1} = \frac{e^2}{2C_1}\,. \qquad \text{(F9)}$$

The Hamiltonian in Eq. (F8) governs the dynamics of the M independent degrees of freedom of the $M+1$ junction system with flux quantization and M identical array junctions. For a two junction system we have $M=1$ and all the sums in Eqs. (F7)-(F8) are absent. Then the Hamiltonian is that given in Eq. (113).

1. Fluxonium

The fluxonium consist of $M+1$ junctions such that a "weak" junction $j=0$ with $E_{J0} < E_{J1}$ is connected to a large array of M junctions ($M \gg 1$) with small phase fluctuations, $E_{C1} \ll E_{J1}$. These conditions enable us to drastically simplify the last two terms of the potential energy $U(\{\phi\})$ for the M independent variables ϕ, ϕ_k $(k=1,\ldots,M-1)$ in Eq. (F7).

We consider small fluctuations of variables ϕ_k around the configuration $\phi_k = 0$, $k=1,\ldots,M-1$, which is an extremum of U for any value of ϕ [as can be checked by differentiating U with respect to ϕ_k and using Eq. (F4)]. We further assume that typical values of ϕ are small compared to $2\pi M$ (note that since M is large, this weak restriction on ϕ and its fluctuations still allows for phase slips through the weak junction). Then we can expand the last two terms in Eq. (F7) to quadratic order in ϕ_k and ϕ/M to find

$$\begin{aligned} U(\{\phi\}) \simeq &- E_{J0}\cos\left(\phi - 2\pi\Phi_e/\Phi_0\right) + \frac{1}{2}E_L\phi^2 \\ &+ \frac{1}{2}E_{J1}\sum_{k=1}^{M-1}\phi_k^2 \end{aligned} \qquad \text{(F10)}$$

with

$$E_L = \frac{E_{J1}}{M}\,. \qquad \text{(F11)}$$

Hence in this approximation the Hamiltonian (F8) for the $M+1$ junction fluxonium separates into independent Hamiltonians for each of the M unconstrained variables ϕ, ϕ_k,

$$H_{\{\phi\}} \;= H_\phi + \sum_{k=1}^{M-1}H_k\,, \qquad \text{(F12)}$$
$$H_\phi \;= 4E_C N^2 - E_{J0}\cos(\phi - 2\pi\Phi_e/\Phi_0) + \frac{1}{2}E_L\phi^2,$$
$$H_k \;= 4E_{C1}N_k^2 + \frac{1}{2}E_{J1}\phi_k^2\,.$$

Up to a change of variable $\phi \to 2\pi\Phi_e/\Phi_0 - \phi$ and redefinitions of symbols, H_ϕ coincides with H_φ of Eq. (2). The relations in Eq. (133) between the parameters of the $M+1$ junctions and the energies E_C and E_L entering the effective qubit Hamiltonian H_ϕ follow from Eqs. (F9) and (F11), respectively.

[1] D. P. DiVincenzo, Fortschr. Phys. **48**, 771 (2000).

[2] J. Koch, T. M. Yu, J. Gambetta, A. A. Houck, D. I. Schuster, J. Majer, A. Blais, M. H. Devoret, S. M. Girvin, and R. J. Schoelkopf, Phys. Rev. A **76**, 042319 (2007).

[3] J. M. Martinis, M. Ansmann, and J. Aumentado, Phys. Rev. Lett. **103**, 097002 (2009).

[4] P. J. de Visser, J. J. A. Baselmans, P. Diener, S. J. C. Yates, A. Endo, and T. M. Klapwijk, Phys. Rev. Lett. **106**, 167004 (2011).

[5] R. M. Lutchyn, L. I. Glazman, and A. I. Larkin, Phys. Rev. B **72**, 014517 (2005).

[6] K. A. Matveev, M. Gisselfält, L. I. Glazman, M. Jonson, and R. I. Shekhter, Phys. Rev. Lett. **70**, 2940 (1993).

[7] P. Joyez, P. Lafarge, A. Filipe, D. Esteve, and M. H. Devoret, Phys. Rev. Lett. **72**, 2458 (1994).

[8] M. H. Devoret and J. M. Martinis, Quant. Inf. Proc. **3**, 163 (2004).

[9] V. E. Manucharyan, J. Koch, M. H. Devoret, and L. I. Glazman, Science **326**, 113 (2009).

[10] G. Catelani, J. Koch, L. Frunzio, R. J. Schoelkopf, M. H. Devoret, and L. I. Glazman, Phys. Rev. Lett. **106**, 077002 (2011).

[11] A. Barone and G. Paternò, *Physics and Applications of the Josephson Effect* (Wiley, New York, 1982).

[12] Note that unity and $\cos\varphi$ in the denominator in Eq. (11) have the same sign, in agreement with Ref. 11. To obtain the correct sign it is important to calculate the matrix element of the time-dependent perturbation in Eq. (8), rather than the matrix element of the tunneling Hamiltonian itself, as was done in Phys. Rev. B **62**, 3040 (2000). The latter procedure leads to the wrong sign for the $\cos\varphi$ term.

[13] C. W. J. Beenakker, in *Transport Phenomena in Mesoscopic Systems*, edited by H. Fukuyama and T. Ando (Springer, Berlin, 1992).

[14] J. Koch, V. E. Manucharyan, M. H. Devoret, and L. I. Glazman, Phys. Rev. Lett. **103**, 217004 (2009).

[15] More precisely, we need to assume that low-lying states in a well are separated from those in nearby wells. This means that we neglect tunneling between wells [which is suppressed when $E_J \gg E_C$, see Eq. (99)]. Tunneling is taken into account in Sec. IV B.

[16] Here and below, in writing the conditions for the validity of our approximations we neglect factors which, for the flux-biased phase qubit, depends on φ_0. This dependence is through trigonometric functions with φ_0 as argument, and for typical flux biases these functions would modify the applicability conditions by factors of order unity. This is consistent with our assumption that the flux is sufficiently far from odd integer multiples of half the flux quantum.

[17] For both the transmon and the flux-biased phase qubit this condition concides, up to numerical factors of order unity, with Eq. (51).

[18] R. M. Lutchyn, L. I. Glazman, and A. I. Larkin, Phys. Rev. B **74**, 064515 (2006).

[19] In the case of the transmon, an estimate for the rate $\Gamma_{1\to 0}$ was given in Eq. (4.10) of Ref. 2 by generalizing the results obtained in Ref. 18 for the Cooper pair box. Note that the present more rigorous treatment gives a parametrically larger rate (by a factor $\sim\sqrt{\Delta/T}$) when applying Eq. (55) to a single junction transmon.

[20] H. Paik, D. I. Schuster, L. S. Bishop, G. Kirchmair, G. Catelani, A. P. Sears, B. R. Johnson, M. J. Reagor, L. Frunzio, L. Glazman, and R. J. Schoelkopf, unpublished [`arXiv:1105.4652`].

[21] M. Lenander, H. Wang, R. C. Bialczak, E. Lucero, M. Mariantoni, M. Neeley, A. D. O'Connell, D. Sank, M. Weides, J. Wenner, T. Yamamoto, Y. Yin, J. Zhao, A. N. Cleland, and J. M. Martinis, Phys. Rev. B (to appear).

[22] R. M. Lutchyn, L. I. Glazman, and A. I. Larkin, Phys. Rev. B **75**, 229903(E) (2007).

[23] We note that in Ref. 14 the limit $E_L \to 0$ was considered at a fixed ratio E_J/E_C.

[24] J. N. L. Connor, T. Uzer, R. A. Marcus, and A. D. Smith, J. Chem. Phys. **80**, 5095 (1984).

[25] The factors in the second line in Eq. (103) were missed in Eq. (22) of Ref. 10. Those factors increase the magnitude of the transition rate but do not affect its functional dependence on flux f.

[26] In this section we neglect for simplicity the dimensionless gate voltage n_g. As discussed in Sec. III, this amounts to neglecting exponentially small corrections, since for both split transmon and fluxonium we consider the regime of Josephson energy large compared to charging energy.

[27] J.Leppäkangas, M. Marthaler, and G. Schön, unpublished [`arXiv:1104.2800`].

[28] A. A. Houck, J. A. Schreier, B. R. Johnson, J. M. Chow, J. Koch, J. M. Gambetta, D. I. Schuster, L. Frunzio, M. H. Devoret, S. M. Girvin, and R. J. Schoelkopf, Phys. Rev. Lett. **101**, 080502 (2008).

[29] Here we neglect for simplicity the renormalization of the parameters that appear in Eq. (102). This is justified since its contribution to the rate can be neglected – see the main text.

[30] In the terms we are neglecting we can distinguish contributions proportional to the distribution function f from a contribution independependent of f. The contribution proportional to f originating from $\delta E_i^{(1),d}$ is logarithmically divergent, but this divergence is cancelled by the similar contribution from $\delta E_i^{(2)}$. The contribution independent of f in $\delta E_i^{(2)}$ is linearly divergent, but independent of the gap Δ; threfore, this divergence can be eliminated by considering energy differences between the superconducting and normal state.

[31] See, e.g., W. A. Harrison, *Solid state theory* (Dover Publications, New York, 1980).

[32] L. D. Landau and E. M. Lifshitz, *Quantum Mechanics* (Butterworth-Heinemann, Oxford, 1981).

[33] W. H. Furry, Phys. Rev. **71**, 360 (1947).

[34] See, e.g., Sec. 28.4 in *Digital Library of Mathematical Functions*, Release date 2010-05-07, National Institute of Standards and Technology, `http://dlmf.nist.gov/`.

[35] Note that the two lowest eigentstates of the reduced Cooper pair box Hamiltonian (75) at $n_g = 1/2$ – see Eqs. (76) and (80) – have the form of the $m = 0$ contributions to the sums in Eq. (C5).

[36] J. A. Schreier, A. A. Houck, J. Koch, D. I. Schuster, B. R. Johnson, J. M. Chow, J. M. Gambetta, J. Majer, L. Frunzio, M. H. Devoret, S. M. Girvin, and R. J. Schoelkopf, Phys. Rev. B **77**, 180502(R) (2008).

[37] L. Sun *et al.*, in preparation.

[38] J. N. Hollenhorst, Phys. Rev. D **19**, 1669 (1979).